SUPPLEMENTARY MATERIALS

A Comparative 'Bottom Up' Proteomics Strategy for the Site-specific Identification and Quantification of Protein Modifications By Electrophilic Lipids

Bingnan Han[1,3], Michael Hare[2], Samanthi Wickramasekara[2], Yi Fang[4] and Claudia S. Maier[1,2]*

[1]Department of Chemistry and [2]Environmental Health Sciences Center

Oregon State University, Corvallis, OR 97331

[3]Department of Ocean Science and Engineering,

Zhejiang University, Hangzhou, China 310028

[4]Department of Agricultural and Biological Engineering,

Purdue University, West Lafayette, IN 47906

Content

Model Protein Data

Mitochondrial Data

Figure S1

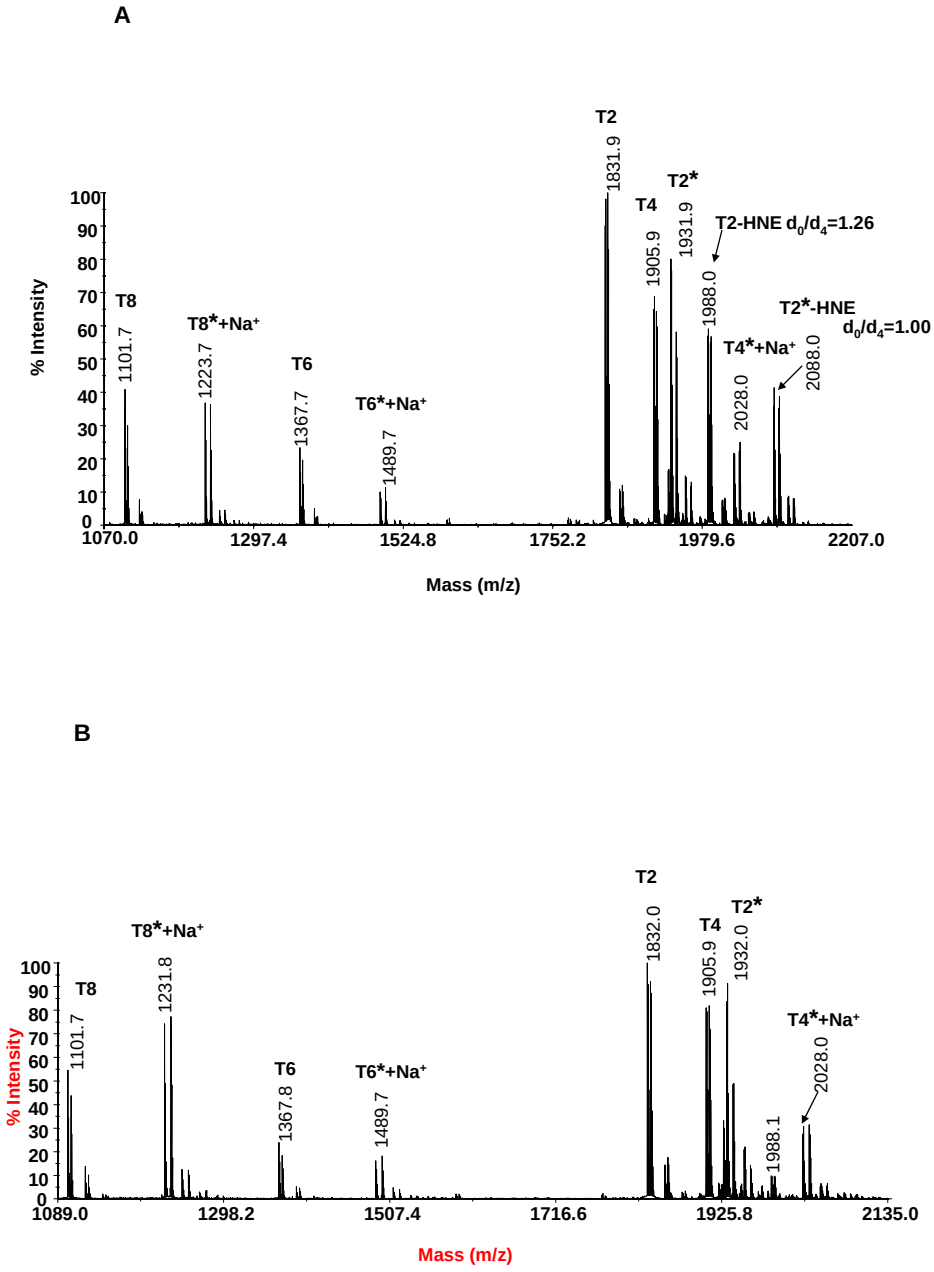
A
% Intensity
Mass (m/z)
T8
1101.7
T8*+Na+
1223.7
T6
1367.7
T6*+Na+
1489.7
T2
1831.9
T4
1905.9
T2*
1931.9
T2-HNE d0/d4=1.26
1988.0
T4*+Na+
2028.0
T2*-HNE
d0/d4=1.00
2088.0
1070.0
1297.4
1524.8
1752.2
1979.6
2207.0
B
% Intensity
Mass (m/z)
T8
1101.7
T8*+Na+
1231.8
T6
1367.8
T6*+Na+
1489.7
T2
1832.0
T4
1905.9
T2*
1932.0
1988.1
T4*+Na+
2028.0
1089.0
1298.2
1507.4
1716.6
1925.8
2135.0

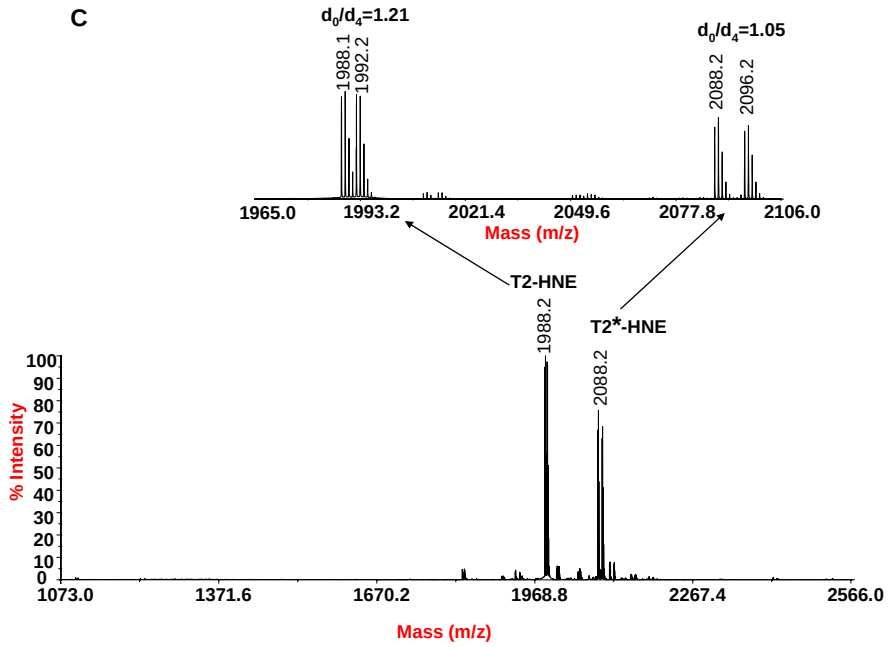

Affinity enrichment of HNE conjugated peptides from the d_0 / d_4- succinic anhydride-labeled tryptic digest of HNE adducted *E. coli* TRX.

(A) MALDI mass spectrum of the unfractionated, d_0 / d_4- succinic anhydride labeled tryptic digest of HNE-modified thioredoxin. The ion pairs at m/z 1988.0, 1992.2 and 2088.0, 2096.2 correlate with tryptic T2-HNE peptides tagged with one or two isotopically labeled succinic anhydrides, respectively.

The following ion pairs containing no HNE were also observed: T2 (1831.9 Da) and T2* (1931.9 Da), IIHLTDDSFDTDVLK; T4 (1905.9 Da) and T4* + Na (2028.0 Da), MIAPILDEIADEYQGK; T6 (1367.7 Da) and T6* + Na (1489.7 Da), LNIDQNPGTAPK; T8 (1101.7 Da) and T8* + Na (1231.8 Da), GIPTLLLFK. The peaks annotated with * represent the bi-succinic anhydride labeled peptide.

(B) MALDI mass spectrum of the capture flow through of the d_0/d_4-succinic anhydride-labeled tryptic digest of HNE adducted *E. coli* TRX.

(C) MALDI mass spectrum of the enriched fraction containing the d_0 / d_4- succinic anhydride -labeled HNE-conjugate of peptides T2-HNE and T2*-HNE. The enriched ion pairs with the expected 1:1 ratio as d_0-and d_4-labeled isotopomeric ion pairs from the crude fraction indicated the specificity of this method.

Figure S2.

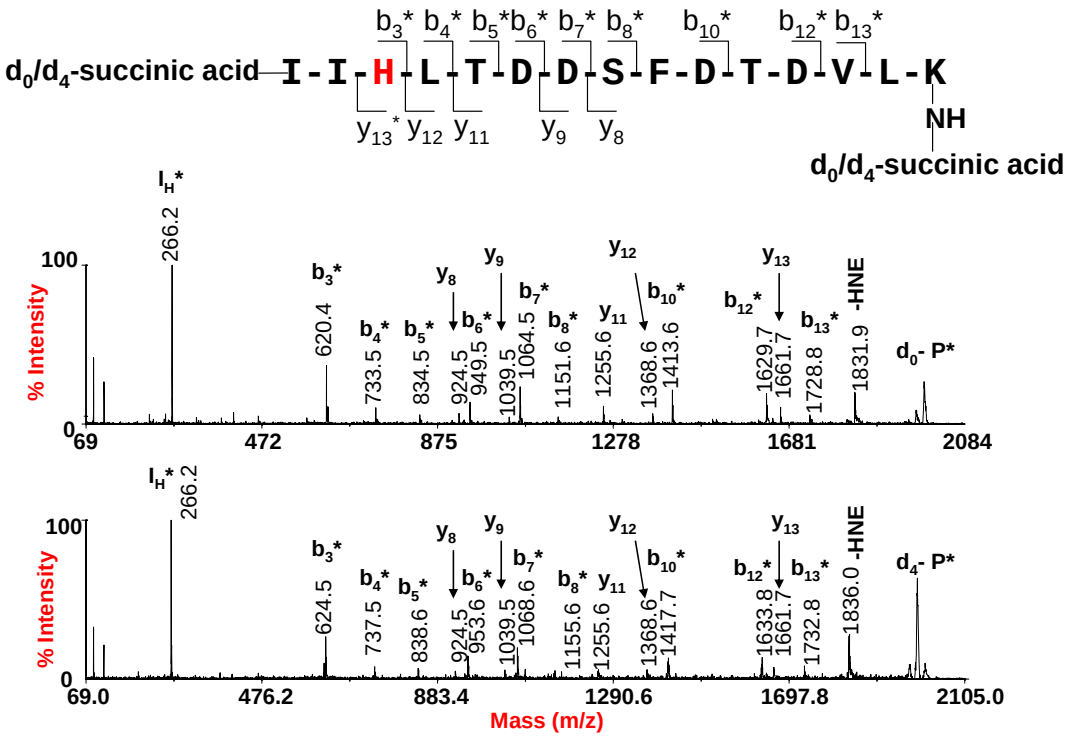

MALDI tandem mass spectrometric identification of the d_0/d_4- succinic anhydride-labeled, HNE-modified peptide T2*-HNE (m/z 2088.0 and 2096.2) from *E.coli* Trx. Fragment ions marked with an asterisk ∗ retained the HNE moiety during high-energy collision induced fragmentation. The ion at m/z 266.2 corresponds to the immonium ion of the HNE-conjugated histidine residue. The prominent ions at m/z 1831.9 and 1836.0 indicate neutral loss of the HNE moiety.

Table S1. Oxylipid peptide conjugates of cardiac mitochondrial proteins identified after Affi-gel Hz enrichment and nanoLC separation. Annotated MALDI tandem mass spectra are shown as supplementary materials, Figure S4-1 through S4-34.

Protein Name	Sprot ID	Peptide sequence and oxylipid modification	MASCOT score	Residue	Figure S3-x
Complex I					
NADH-ubiquinone oxidoreductase 51 kDa subunit	NUBM_RAT	NAC*GSDYDFDVFVVR[b]	87	C^{187}	1
		LVEGC*LVGGR[a]	35	C^{142}	2
		LFNISGHVNHPC*TVEEEMSVPLK[a]	19	C^{286}	3
NADH-ubiquinone oxidoreductase 75 kDa subunit	NUAM_RAT	VDSDNLC*TEEIFPTEGAGTDLR[a]	54	C^{367}	4
NADH-ubiquinone oxidoreductase 9.6kDa subunit	ACPM_MOUSE	LMC*PQEIVDYIADKK[a]	76	C^{140}	5
NADH-ubiquinone oxidoreductase chain 3	NU3M_RAT	ANPYEC*GFDPTSSAR[a]	50	C^{39}	6
NADH dehydrogenase 1 alpha subcomplex subunit 5	NDUA5_RAT	TTGLVGLAVC*DTPHER[a]	41	C^{16}	7
NADH dehydrogenase 1 alpha subcomplex subunit 6	NDUA6_MOUSE	FFH*ETETPRPK[b]	21	H^{111}	8
NADH dehydrogenase 1 alpha subcomplex subunit 7	NDUA7_MOUSE	LSNNYYC*TR[a]	37	C^{54}	9
Complex II					
Succinate dehydrogenase [ubiquinone] flavoprotein subunit	DHSA_RAT	TYFSC*TSAHTSTGDGTAMVTR[a,d]	92	C^{258}	10,11
		GVIALC*IEDGSIHR[a]	31	C^{238}	12
		TLNEADC*ATVPPAIR[a]	54	C^{646}	13
Complex III					
Ubiquinol-cytochrome-c reductase complex core protein I	UQCR1_MOUSE	NALISH*LDGTTPVC*EDIGR[a,b]	56	H^{402}, C^{410}	14
		NALISHLDGTTPVC*EDIGR[a]	45	C^{410}	15

Ubiquinol-cytochrome-c reductase complex core protein II	UQCR2_RAT	NALANPLYC*PDYR[a,b,c,d]	66	C^{191}	16-19
Cytochrome c1, heme protein, mitochondrial	CY1_MOUSE	HLVGVC*YTEEEAK[a]	86	C^{139}	20
Complex IV					
Cytochrome c oxidase subunit VIa isoform 2	CX6A2_RAT	GDH*GGAGANTWR[b,c]	28	H^{20}	21,22
		HNPH*VNPLPTGYEQP[b]	35	H^{83}	23
Cytochrome c oxidase subunit VIb isoform 1	CX6B1_RAT	GGDVSVC*EWYR[b]	23	C^{53}	24
Cytochrome c oxidase subunit VIIa isoform 2	CX7A2_RAT	LFQEDNGMPVH*LK[b]	42	H^{44}	25
Complex V					
ATP synthase beta subunit	ATPβ_RAT	IMDPNIVGSEH*YDVAR[b]	81	H^{417}	26
ATP synthase O subunit	ATPO_RAT	GEVPC*TVTTAFPLDEAVLSELK[a]	72	C^{141}	27
Citric Acid Cycle					
Aconitate hydratase	ACON_RAT	VAVPSTIH*CDHLIEAQLGGEK[a]	30	H^{125}	28
Malate dehydrogenase	MDHM_RAT	GYLGPEQLPDC*LK[a]	37	C^{89}	29
ß-Oxidation					
Long-chain fatty-acid-CoA ligase 1	ACSL1_RAT	GIQVSNDGPC*LGSR[a]	28	C^{109}	30
Other					
ADP/ATP translocase 1	ADT1_RAT	GADIMYTGTVDC*WR[a,b]	79	C^{256}	31,32
		EFNGLGDC*LTK[a]	61	C^{159}	33
Voltage-dependent anion-selective channel protein 1	VDAC1_RAT	EHINLGC*DVDFDIAGPSIR[a]	68	C^{140}	34

[1] The site of oxylipid conjugation is marked with an asterisk (*). The chemical nature of the oxylipid modification is indicated by the following superscripts: a, acrolein, b, HHE, c, ONE, d, HNE.

Table S2. Identified oxylipid peptide conjugates of cardiac mitochondrial proteins after post-digestion labeling with succinic anhydride, Affi gel-Hz enrichment and nanoLC MALDI tandem mass spectrometry.

Protein Name	Sprot ID	Peptide sequence	MASCOT score	Residue
Complex I				
NADH-ubiquinone oxidoreductase 13 kDa-A subunit	NUMM_MOUSE	ITH*TGQVYDEK[b]	70	H[33]
NADH dehydrogenase [ubiquinone] iron-sulfur protein 3	NDUS3_MOUSE	ILTDYGFEGH*PFR[b]	28	H[195]
NADH-ubiquinone oxidoreductase 75 kDa subunit	NDUS1_RAT	VDSDNLC*TEEIFPTEGAGTDLR[b]	81	C[367]
NADH dehydrogenase 1 alpha subcomplex subunit 5	NDUA5_RAT	TTGLVGLAVC*DTPHER[a]	51	C[16]
NADH dehydrogenase 1 alpha subcomplex subunit 10	NDUAA_MOUSE	KQC*VDHYNEIK[a]	78	C[183]
Complex II				
Succinate dehydrogenase [ubiquinone] flavoprotein subunit	DHSA_RAT	GVIALC*IEDGSIHR[a]	33	C[238]
		TYFSC*TSAHTSTGDGTAMVTR[a]	124	C[258]
		TLNEADC*ATVPPAIR[a,b]	68	C[646]
Succinate dehydrogenase [ubiquinone]iron-sulfur protein	DHSB_MOUSE	IK*NEVDSTLTFR[b]	38	K[82]
Complex III				
Ubiquinol-cytochrome-c reductase complex core protein I	UQCR1_MOUSE	NALISHLDGTTPVC*EDIGR[a,b]	73	C[410]
		YFYDQC*PAVAGYGPIEQLSDYNR[b]	33	C[453]
Ubiquinol-cytochrome-c reductase complex core protein II	UQCR2_RAT	NALANPLYC*PDYR[a,b,c,d]	77	C[191]
Cytochrome c1, heme protein, mitochondrial	CY1_MOUSE	HLVGVC*YTEEEAK[a]	117	C[139]
Complex IV				
Cytochrome c oxidase subunit VIa isoform 2	CX6A2_RAT	GDH*GGAGANTWR[a,b,c]	88	H[20]
Cytochrome c oxidase subunit VIb isoform 1	CX6B1_RAT	GGDVSVC*EWYR[b]	28	C[53]
Cytochrome c oxidase subunit VIIa isoform 2	CX7A2_RAT	LFQEDNGMPVH*LK[b]	51	H[44]
Cytochrome c oxidase subunit 4 isoform 1	COX41_RAT	DYPLPDVAH*VK[b]	41	H[51]
Cytochrome c oxidase subunit 3	COX3_RAT	EGTYQGHH*TPIVQK[b]	56	H[71]
Cytochrome c oxidase polypeptide VIIc	COX7C_RAT	SH*YEEGPGK[b]	41	H[18]

Complex V				
ATP synthase beta subunit	ATPβ_RAT	IMDPNIVGSEH*YDVAR[b, c]	71	H[417]
		EGNDLYH*EMIESGVINLK[b]	71	H[248]
ATP synthase B chain	AT5F1_RAT	EGEH*MINWVEK[b]	42	H[214]
Citric Acid Cycle				
Malate dehydrogenase	MDHM_RAT	VNVPVIGGH*AGK[b]	30	H[200]
Isocitrate dehydrogenase [NADP]	IDHP_RAT	HAH*GDQYK[b]	41	H[247]
Creatine kinase, sarcomeric mitochondrial precursor	KCRS_RAT	ITH*GQFDER[b]	29	H[152]
ß-Oxidation				
Long-chain specific acyl-CoA dehydrogenase	ACADL_RAT	C*IGAIAMTEPGAGSDLQGVR[b]	40	C[166]
		AFVDSC*LQLHETK[a]	81	C[351]
Acetyl-CoA acetyltransferase	THIL_RAT	IHMGNC*AENTAK[a]	45	C[193]
Other				
ADP/ATP translocase 1	ADT1_RAT	GADIMYTGTVDC*WR[a,b]	48	C[256]
		LLLQVQH*ASK[b]	72	H[39]
NAD(P) transhydrogenase, mitochondrial precursor	NNTM_MOUSE	AISPDKDNFH*FEVK[b]	40	H[407]
		GITH*IGYTDLPSR[b]	40	H[370]

[1] The site of oxylipid conjugation is marked with an asterisk (*). The chemical nature of the oxylipid modification is indicated by the following superscripts: a, acrolein, b, HHE, c, ONE, d, HNE.

Table S3. Comparison of experimental *vs* expected d_0/d_4 ratios for oxylipid peptide conjugates from 1:1 mixtures of mitochondrial proteome preparations. After post-digestion labeling with d_0- and d_4-succinic anhydride, respectively, labeled mixtures were combined, subjected to AffiGel-Hz enrichment and analyzed by nanoLC MALDI-MS/MS.

Sprot ID	**Peptide sequence[1]**	**d_0 / d_4 (Expected Ratio = 1.00), n=3**					
		sample 1	**sample 2**	**sample 3**	**Average**	**±**	**SD**
NDUA5_RAT	TTGLVGLAVC*DTPHER[a]	0.84	0.97	0.85	0.89	±	0.07
DHSA_RAT	TLNEADC*ATVPPAIR[a]	1.15	1.23	1.05	1.14	±	0.09
	TYFSC*TSAHTSTGDGTAMVTR[a]	1.04	1.08	1.09	1.07	±	0.03
UQCR2_RAT	NALANPLYC*PDYR[a]	1.23	1.05	1.12	1.13	±	0.09
	NALANPLYC*PDYR[b]	0.97	0.95	1.01	0.98	±	0.03
CX6A2_RAT	GDH*GGAGANTWR[a]	1.17	1.05	1.04	1.09	±	0.07
	GDH*GGAGANTWR[b]	0.96	0.99	1.01	0.99	±	0.03
	GDH*GGAGANTWR[c]	0.91	0.96	1.24	1.04	±	0.18
CX7A2_RAT	LFQEDNGMPVH*LK[b]	1.00	1.02	0.85	0.96	±	0.09
COX41_RAT	DYPLPDVAH*VK[b]	0.90	1.05	0.98	0.98	±	0.08
COX3_RAT	EGTYQGHH*TPIVQK[b]	1.48	1.00	1.03	1.17	±	0.27
CX6B1_RAT	GGDVSVC*EWYR[b]	1.05	1.01	0.96	1.01	±	0.05
ATPβ_RAT	IMDPNIVGSEH*YDVAR[b]	1.15	1.05	1.02	1.07	±	0.07
KCRS_RAT	ITH*GQFDER[b]	0.97	0.90	0.96	0.94	±	0.04
MDHM_RAT	GC*DVVVIPAGVPR[b]	0.96	1.26	1.03	1.08	±	0.16
ACADL_RAT	C*IGAIAMTEPGAGSDLQGVR[b]	1.13	1.02	1.04	1.06	±	0.06
ADT1_RAT	GADIMYTGTVDC*WR[a]	0.93	0.93	1.11	0.99	±	0.10
	GADIMYTGTVDC*WR[b]	1.05	1.11	1.01	1.06	±	0.05
	LLLQVQH*ASK[b]	0.96	1.06	0.90	0.97	±	0.08
Average ± SD		1.04 ± 0.15	1.04 ± 0.09	1.02 ± 0.09	1.03	±	0.07

[1] The site of oxylipid conjugation is marked with an asterisk (*). The chemical nature of the oxylipid modification is indicated by the following superscripts: a, acrolein, b, HHE, c, ONE, d, HNE

Figure S3-1
4700 MS/MS Precursor 1820.81

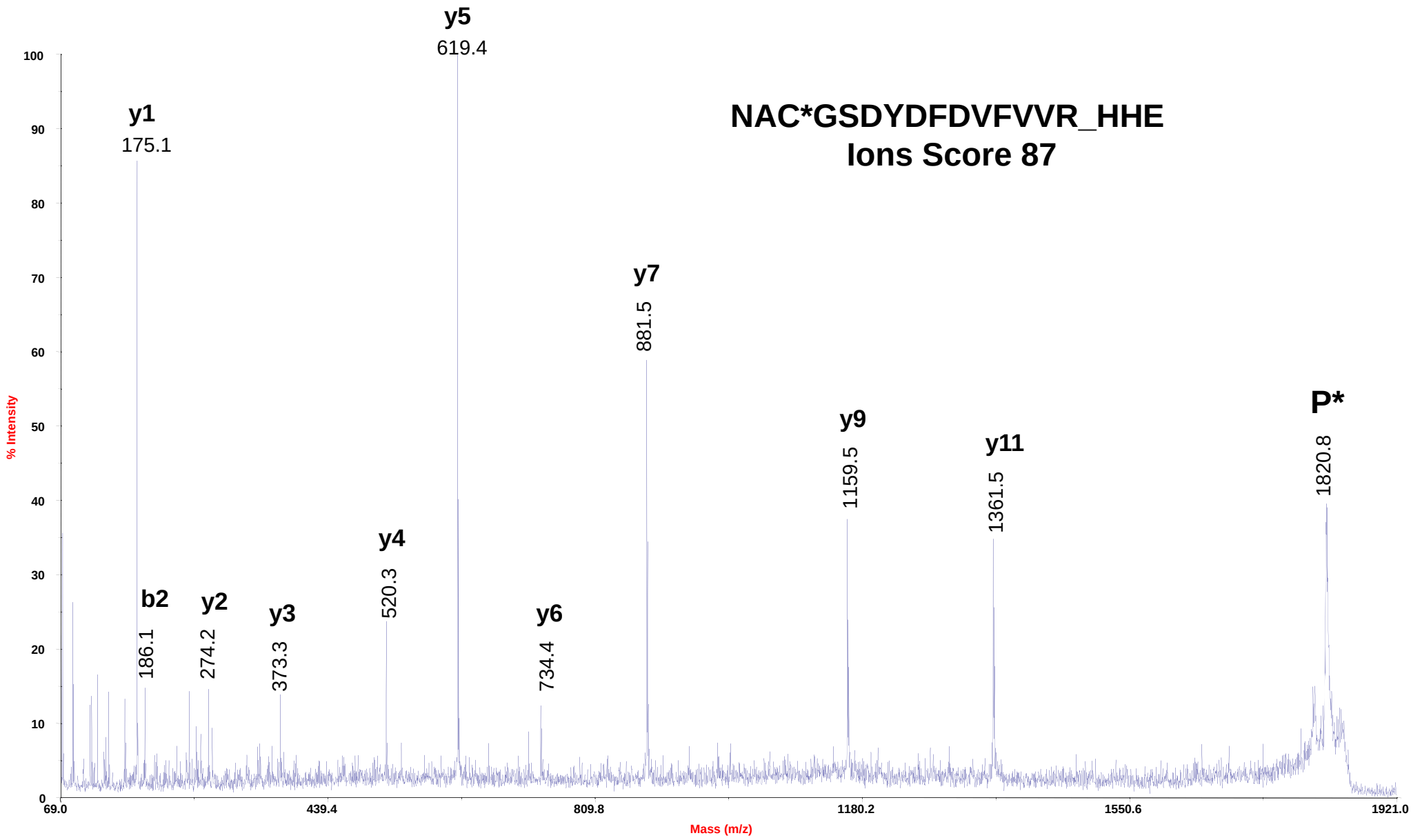

Figure S3-2
4700 MS/MS Precursor 1058.62

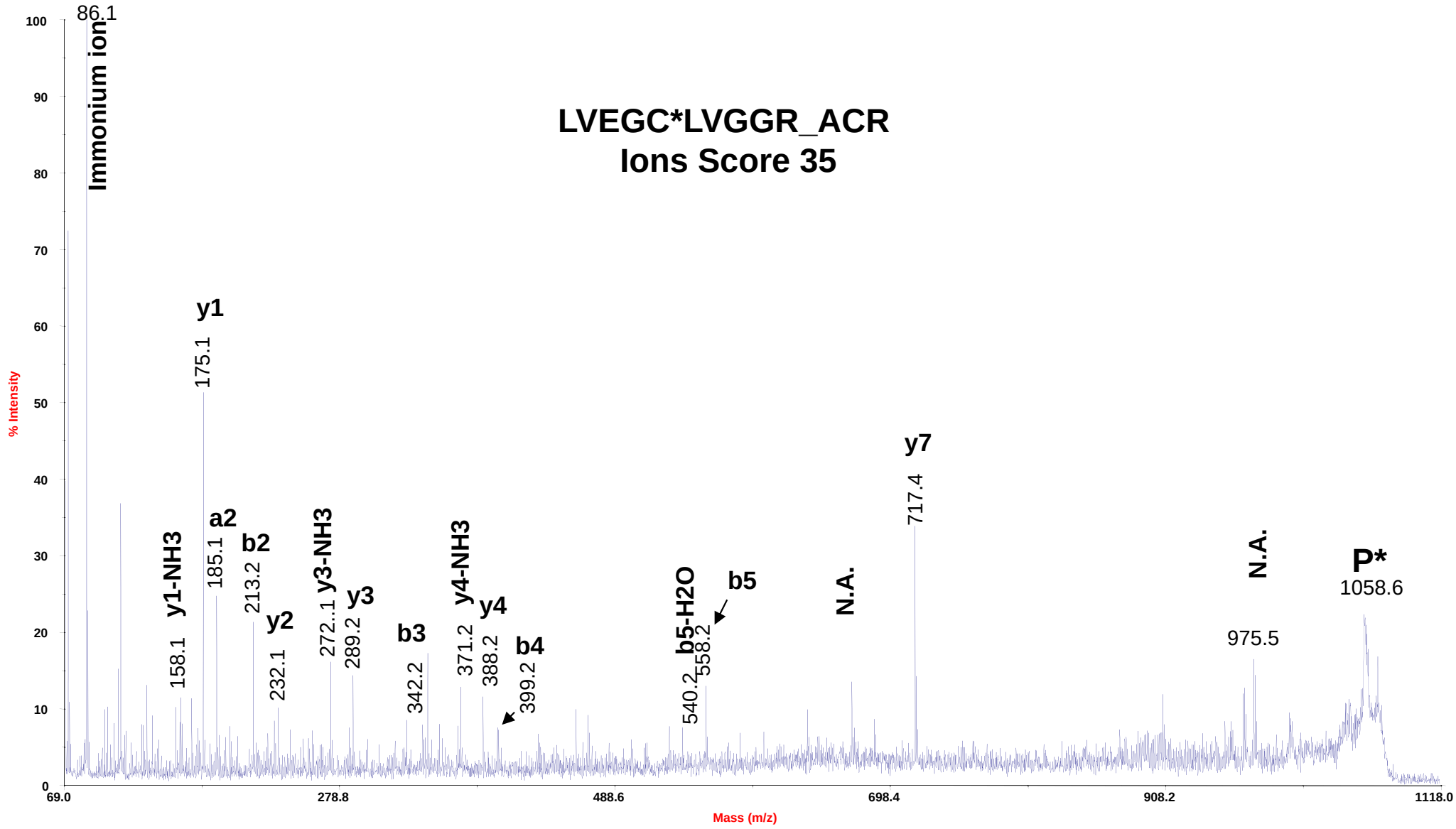

Figure S3-3
4700 MS/MS Precursor 2636.37

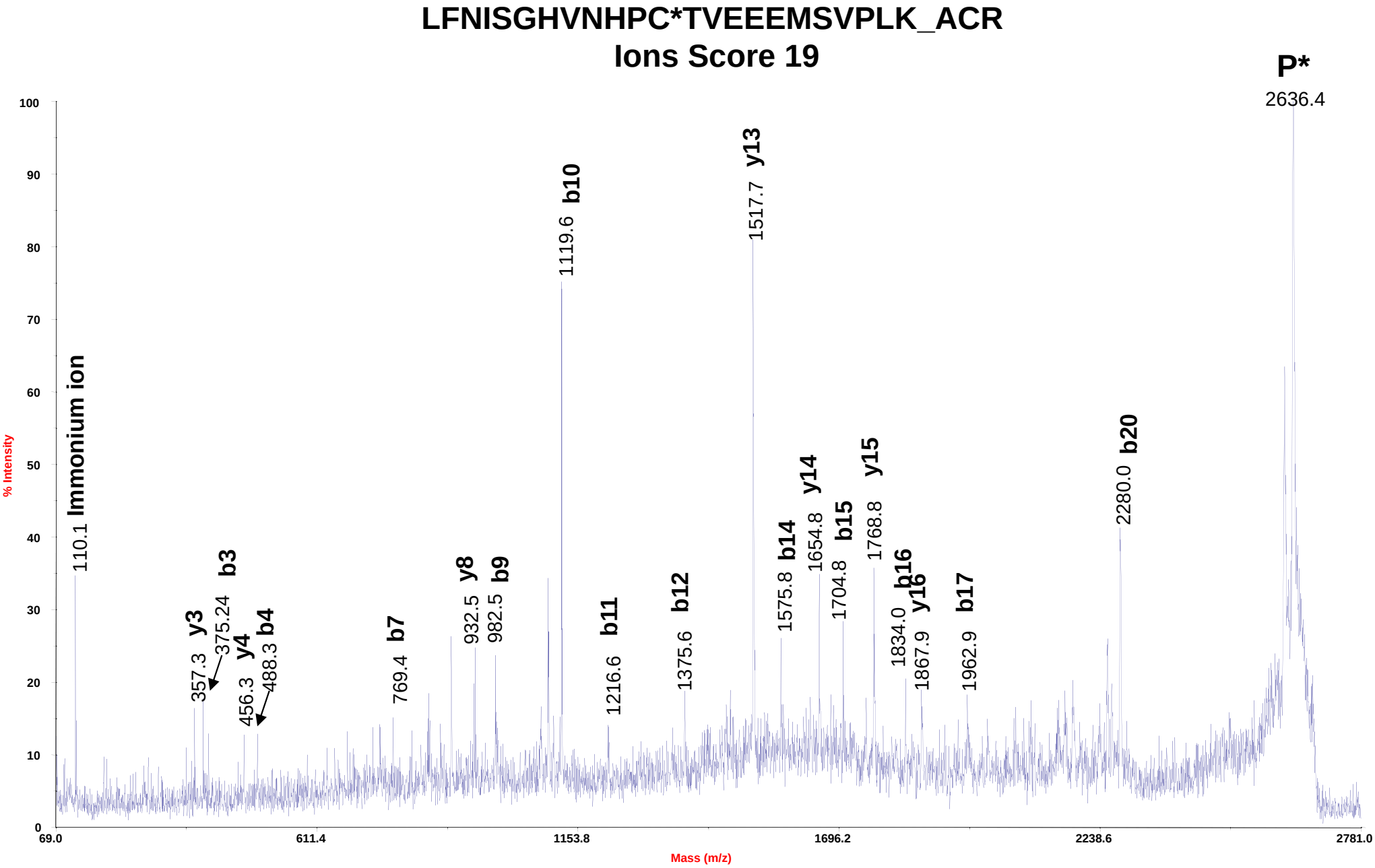

Figure S3-4
4700 MS/MS Precursor 2438.24

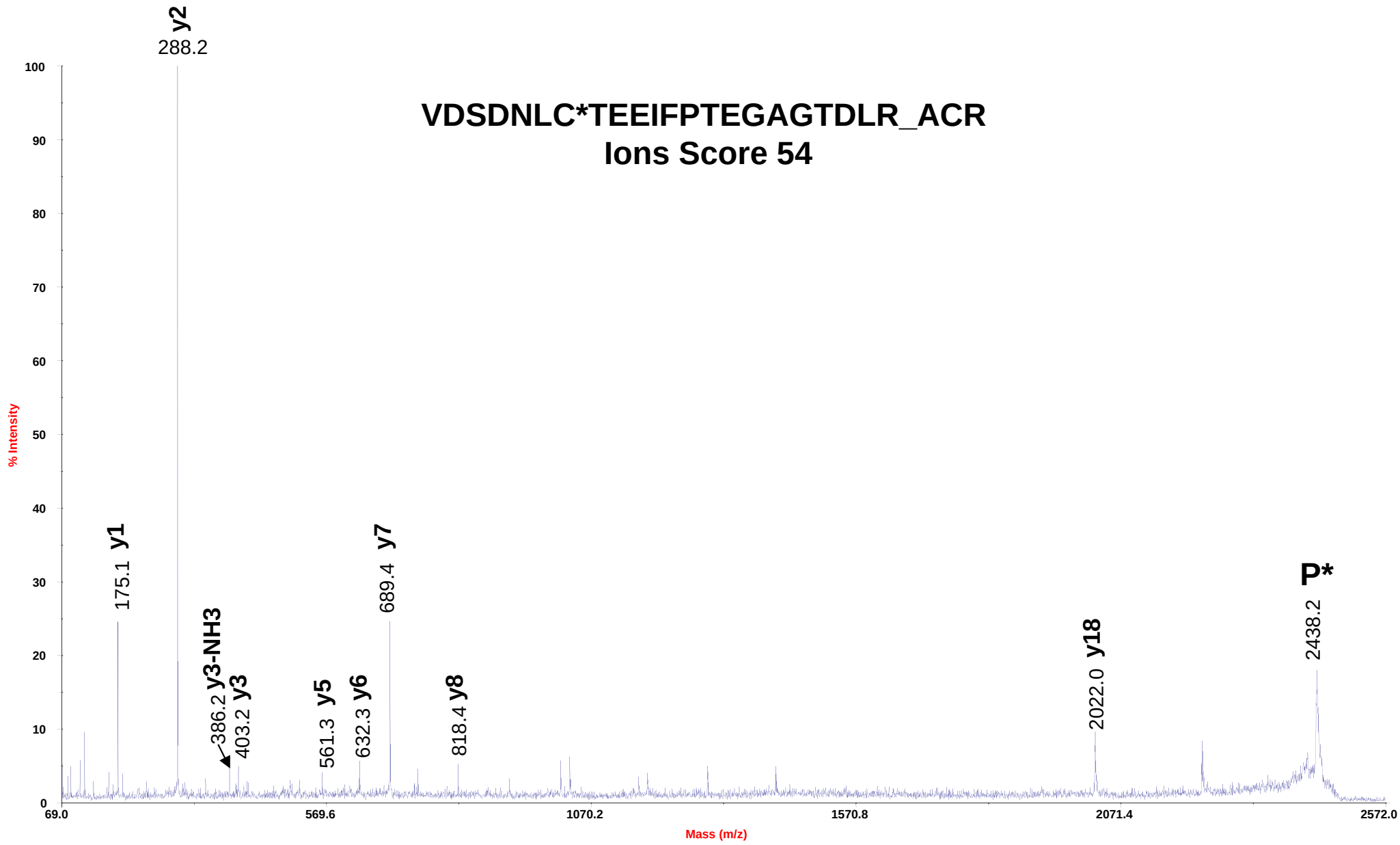

Figure S3-5
4700 MS/MS Precursor 1821.94

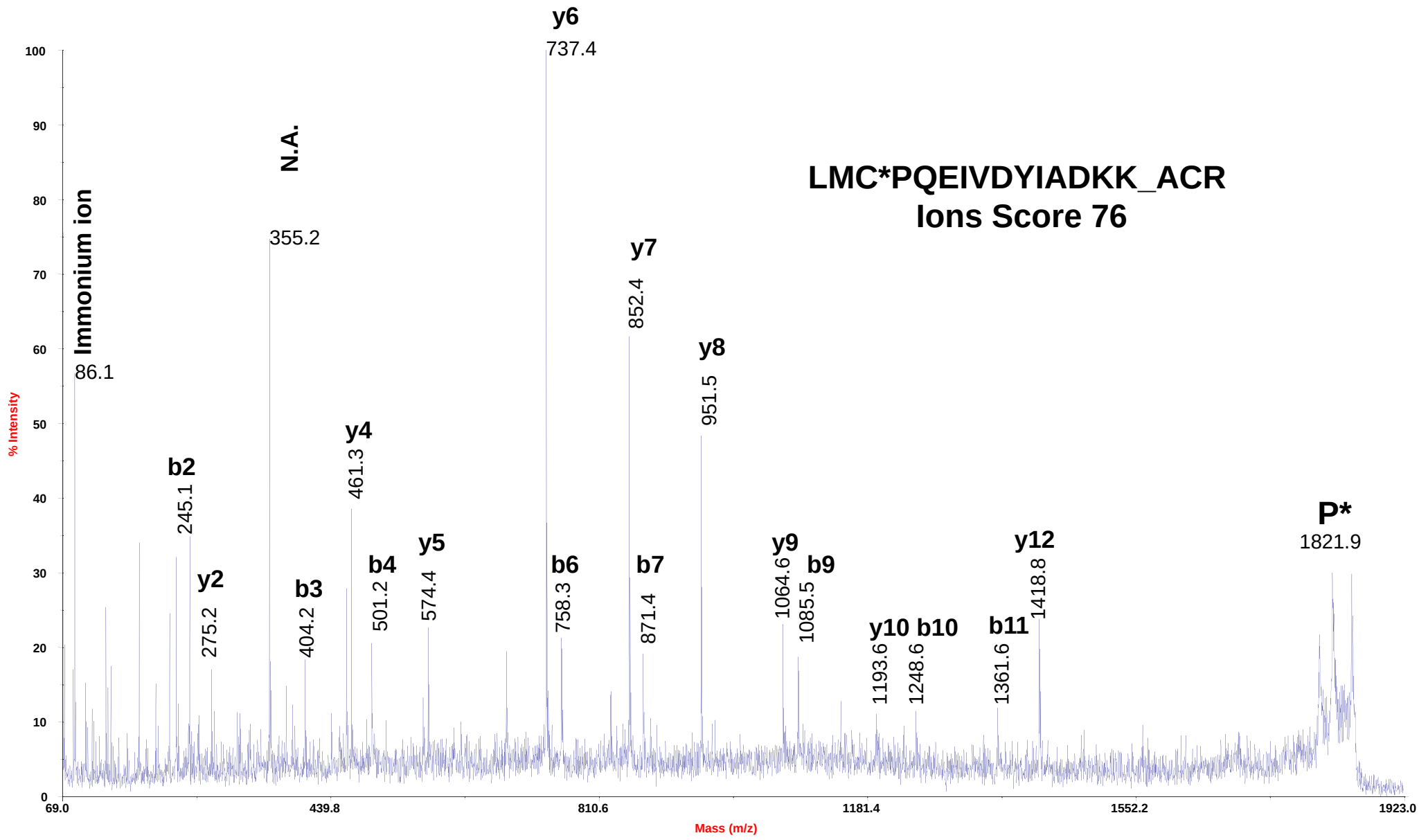

Figure S3-6
4700 MS/MS Precursor 1670.78

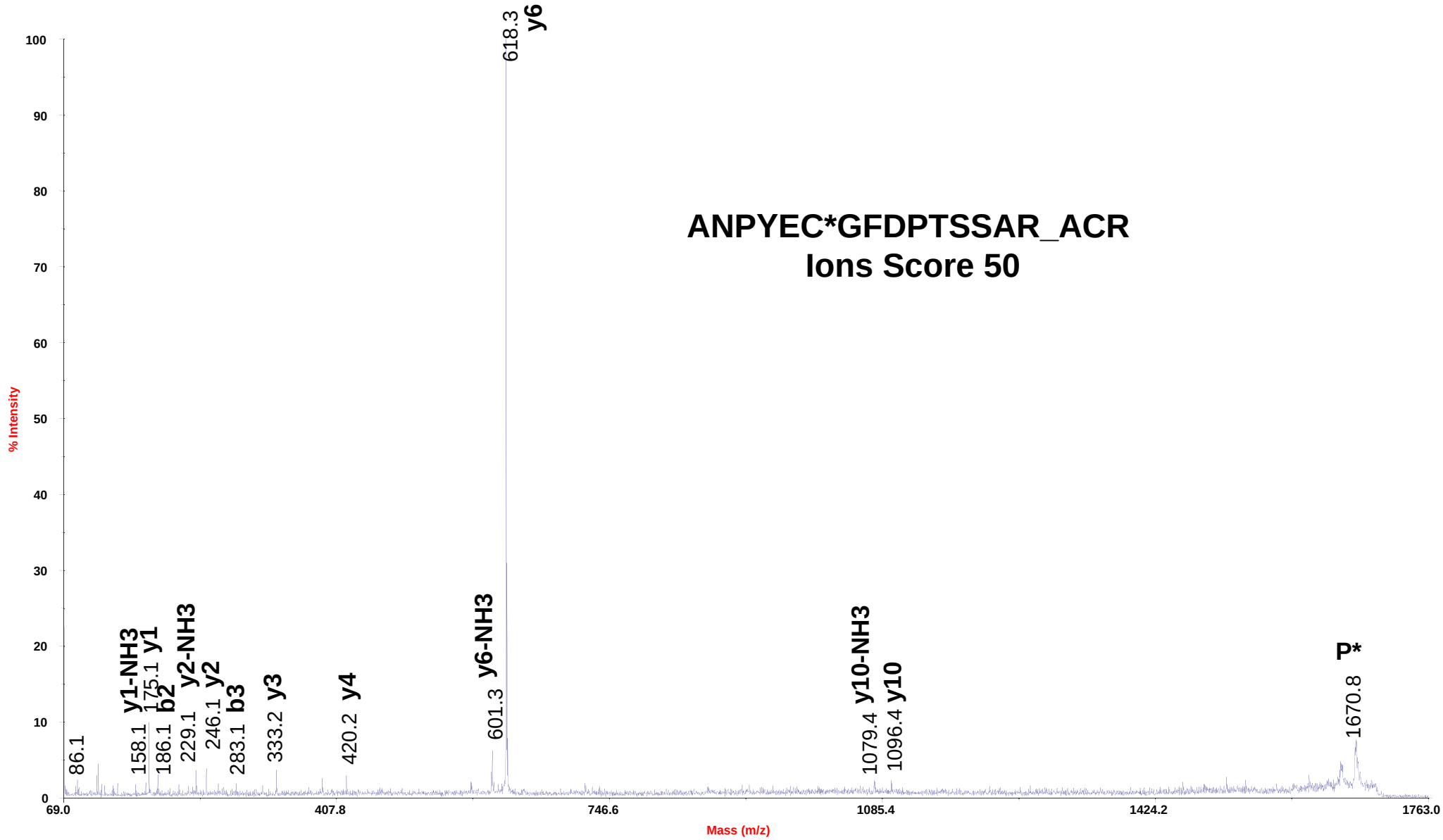

Figure S3-7
4700 MS/MS Precursor 1724.96

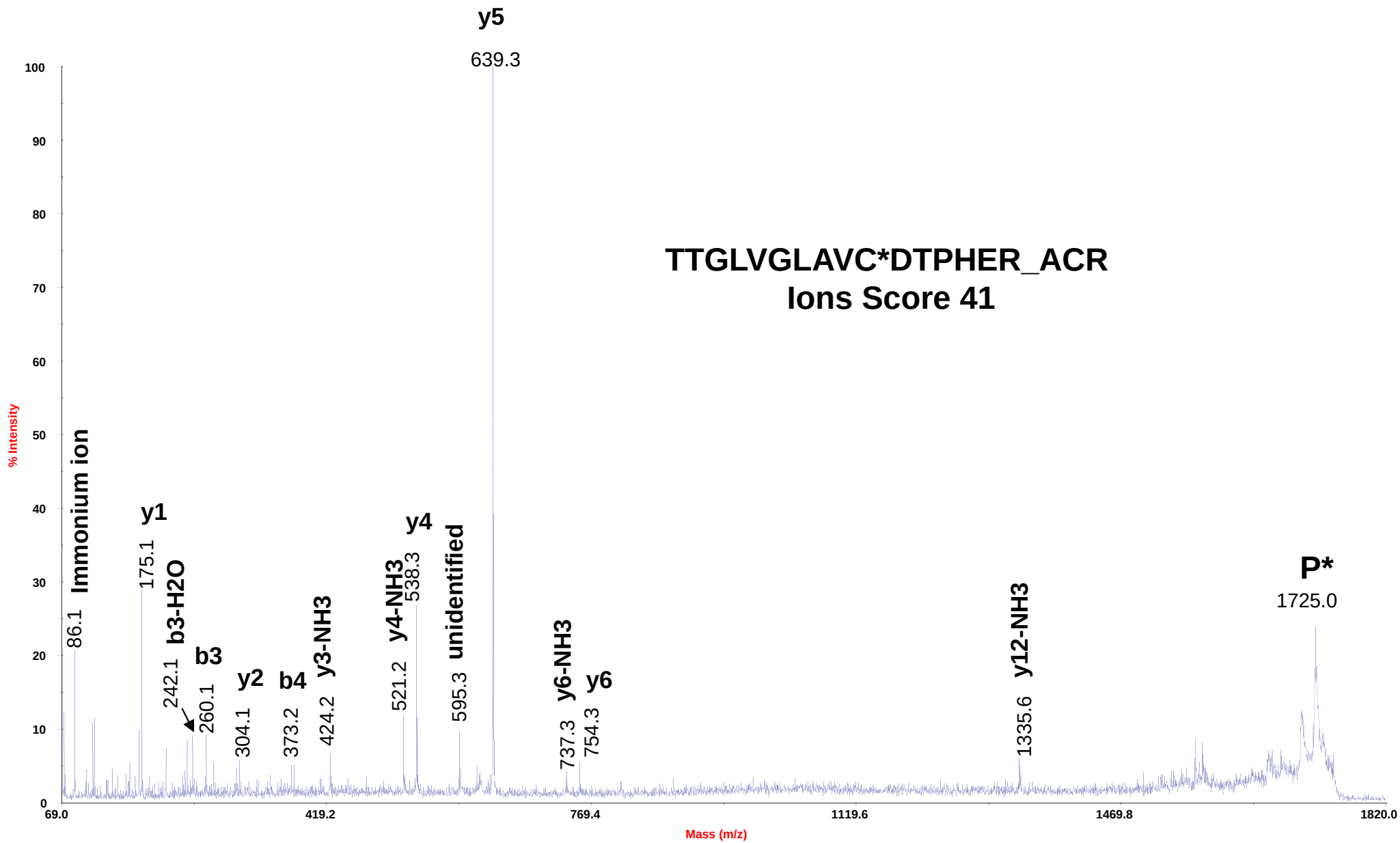

Figure S3-8
4700 MS/MS Precursor 1502.73]

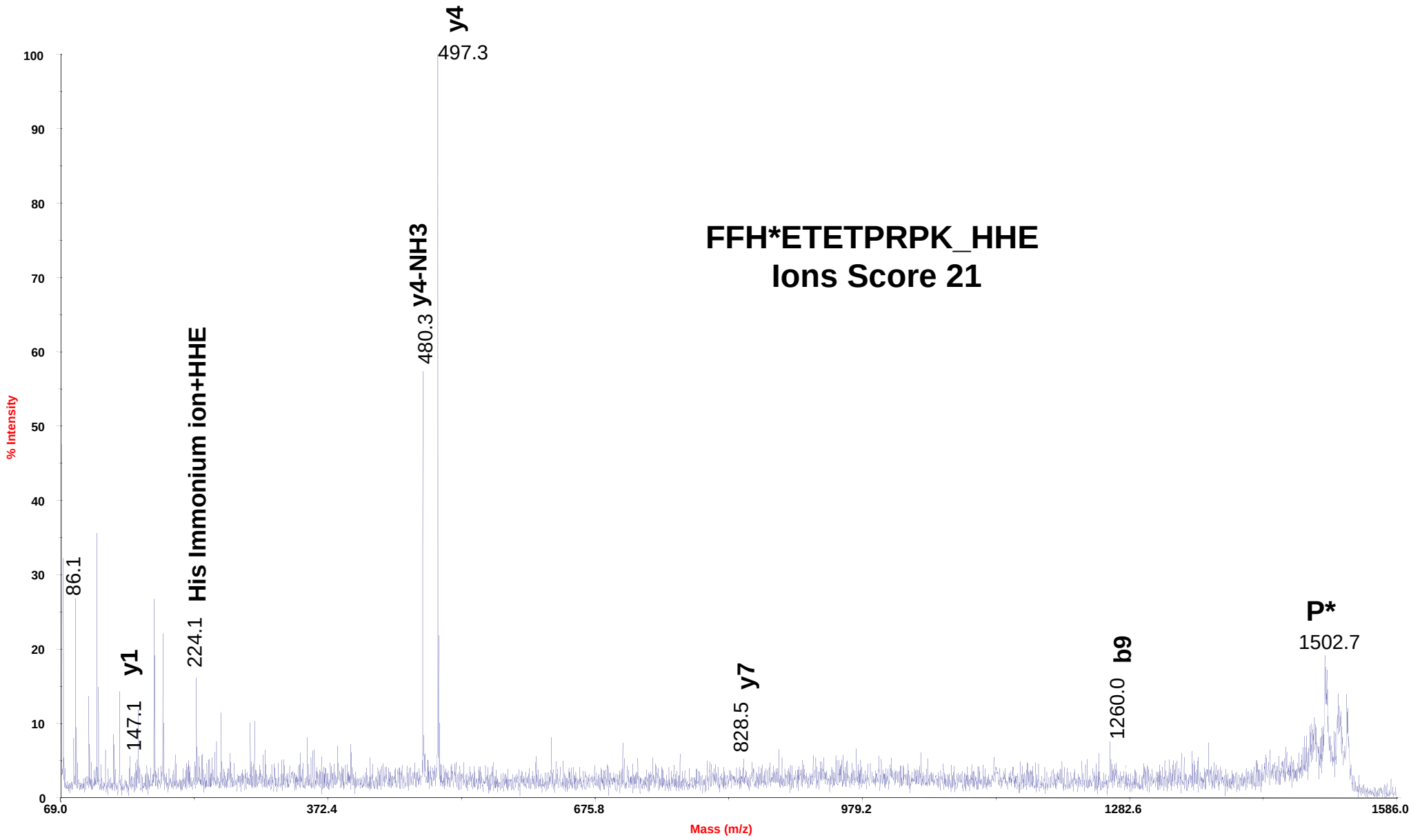

Figure S3-9
4700 MS/MS Precursor 1189.59

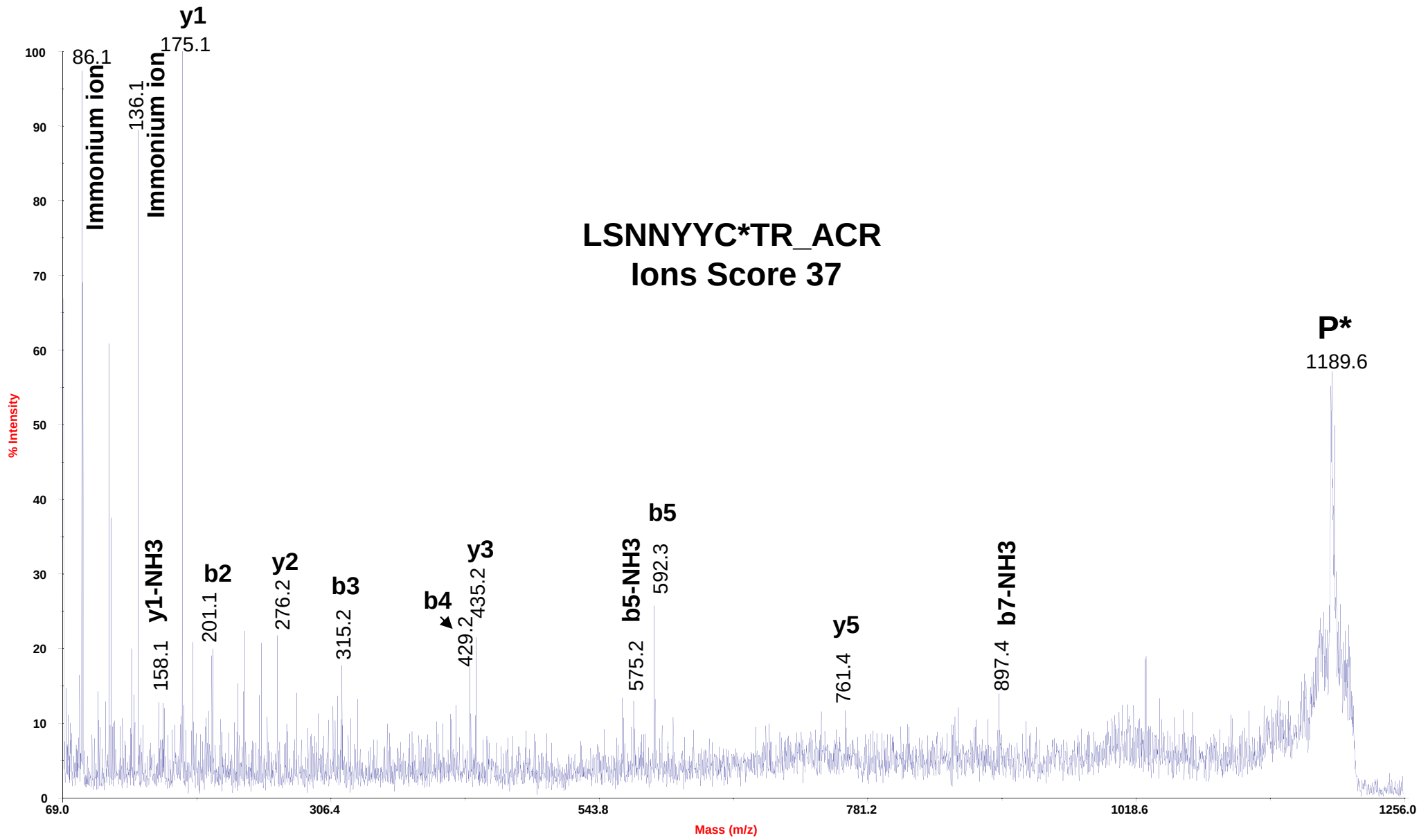

Figure S3-10
4700 MS/MS Precursor 2249.95

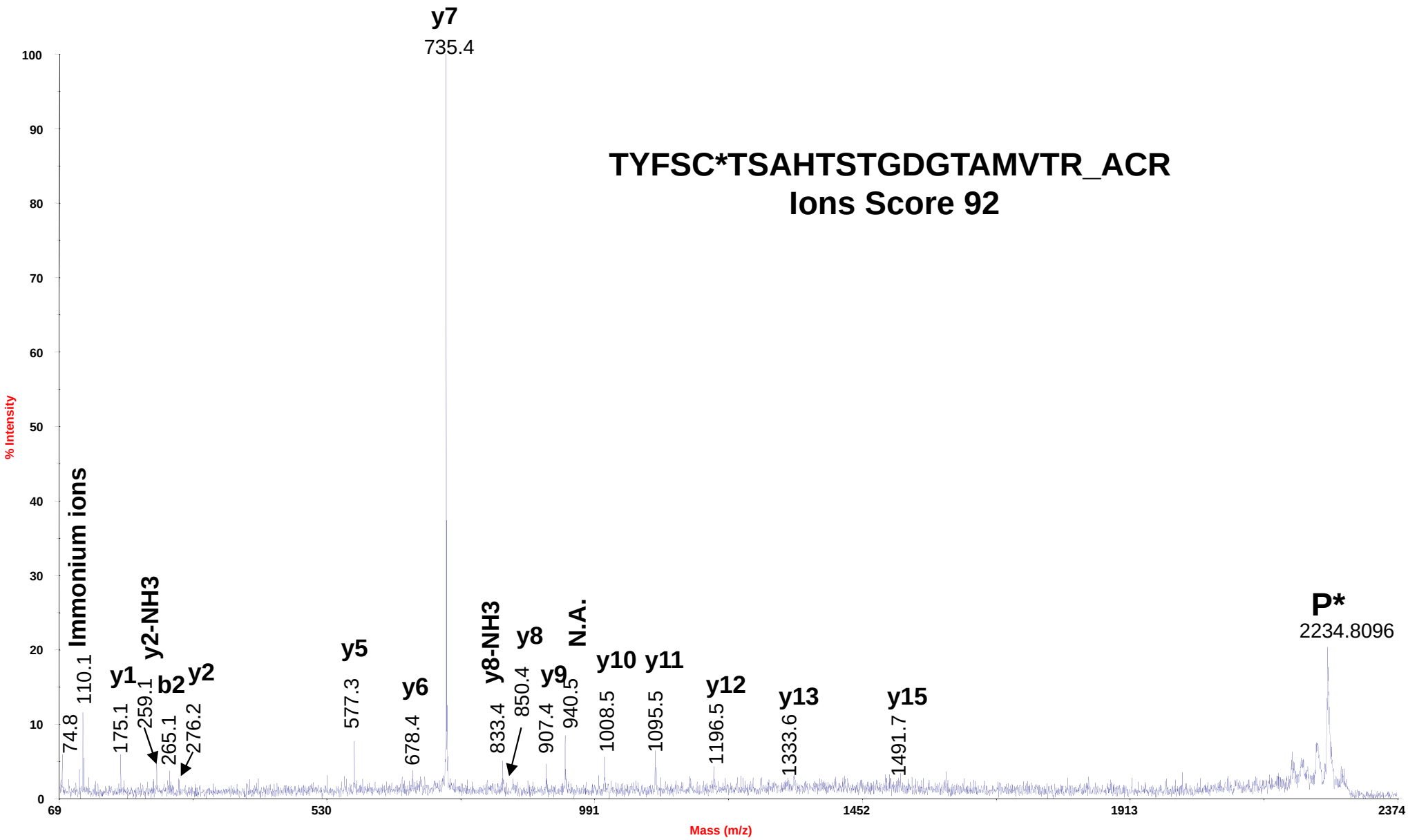

Figure S3-11
4700 MS/MS Precursor 2350.12

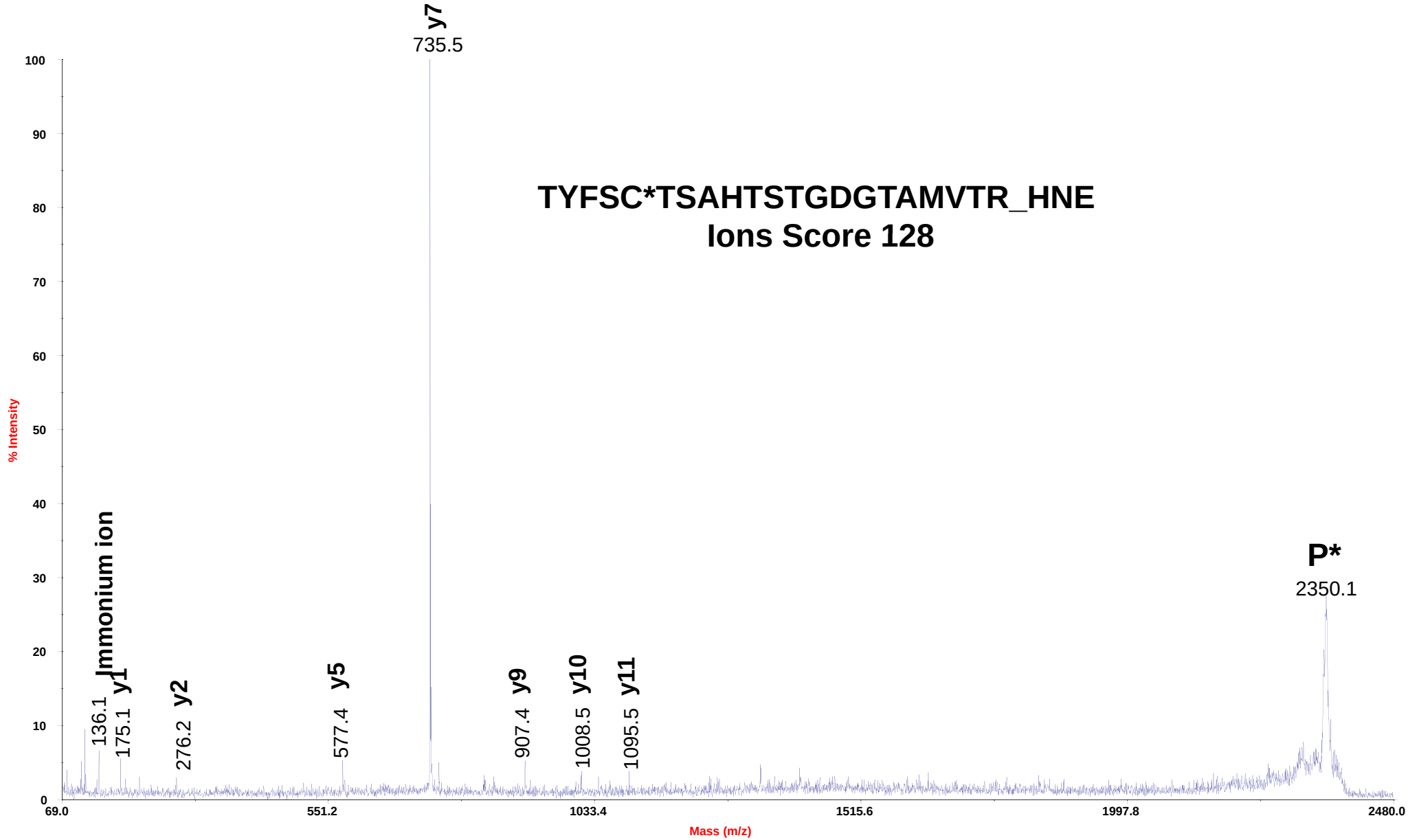

Figure S3-12
4700 MS/MS Precursor 1538.81

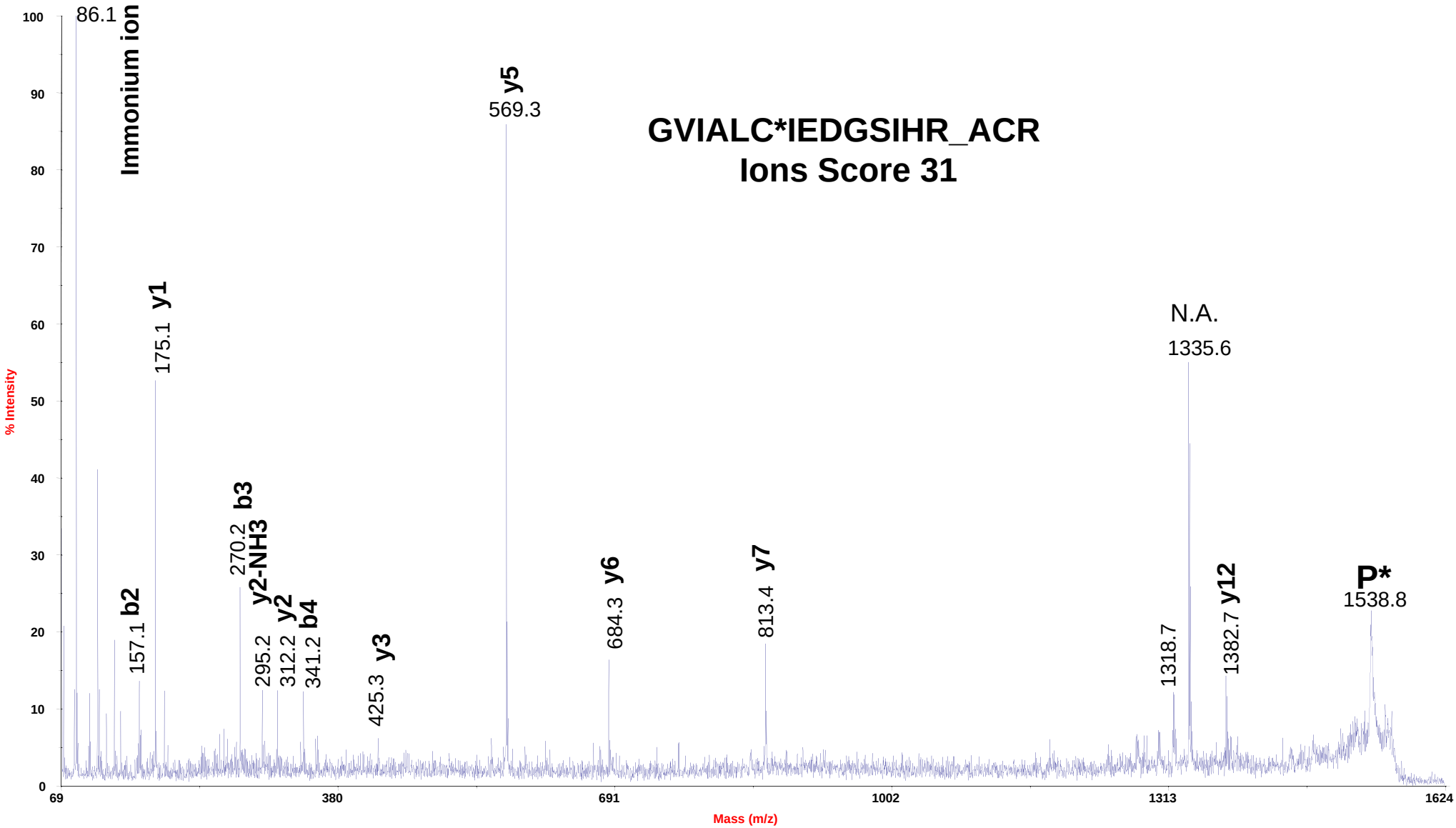

Figure S3-13
4700 MS/MS Precursor 1626.88

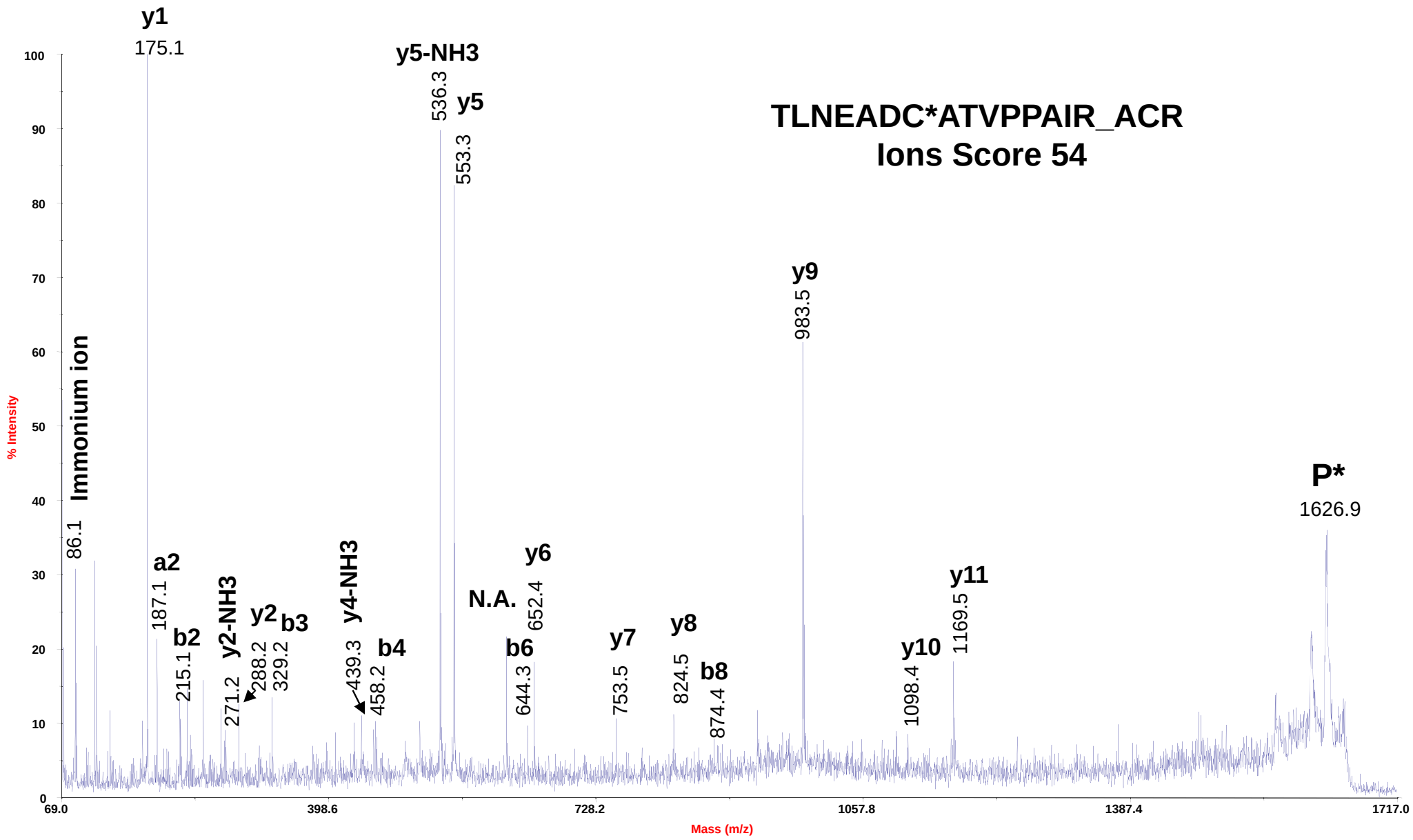

Figure S3-14
4700 MS/MS Precursor 2167.2

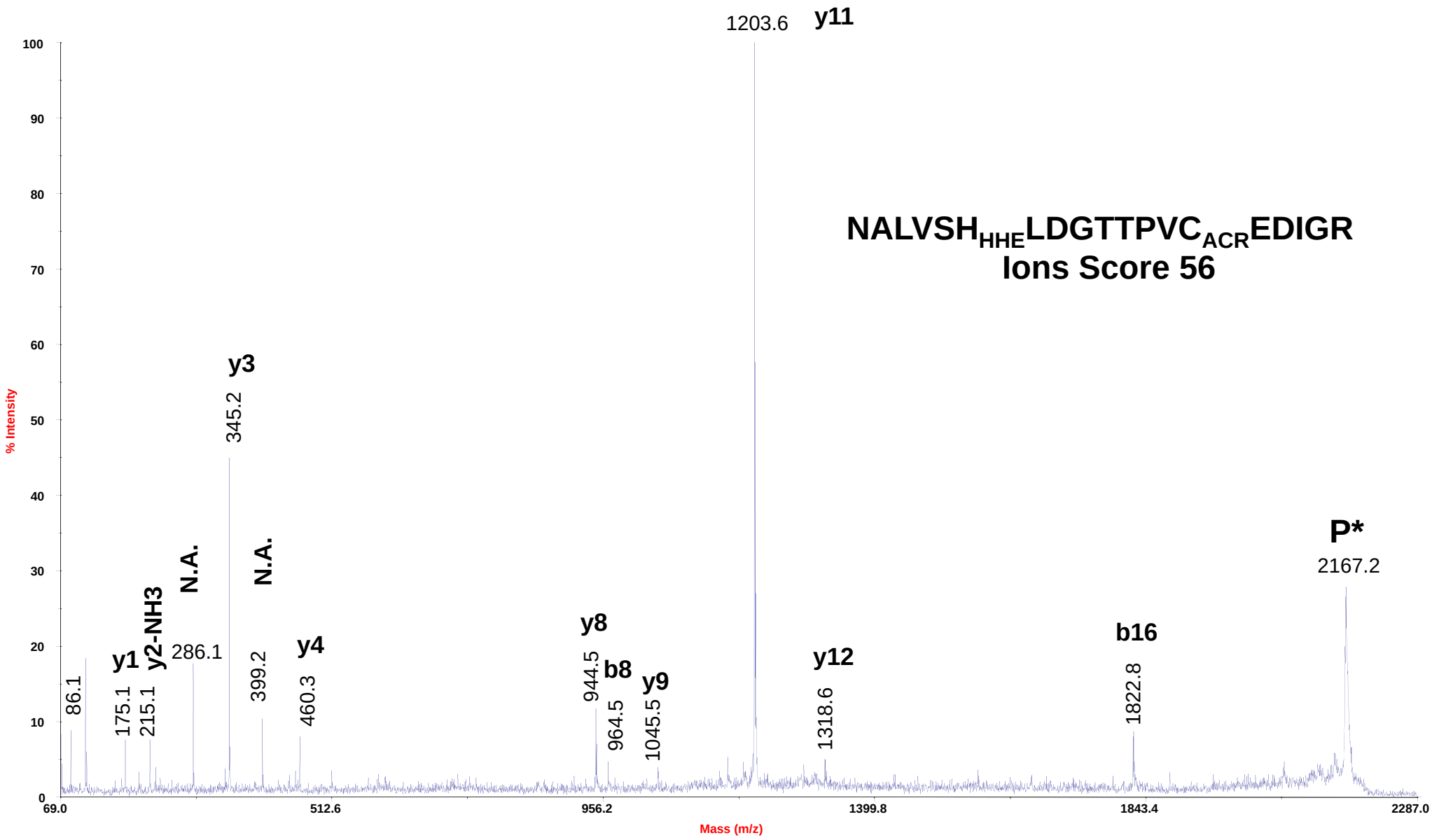

Figure S3-15
4700 MS/MS Precursor 2067.05

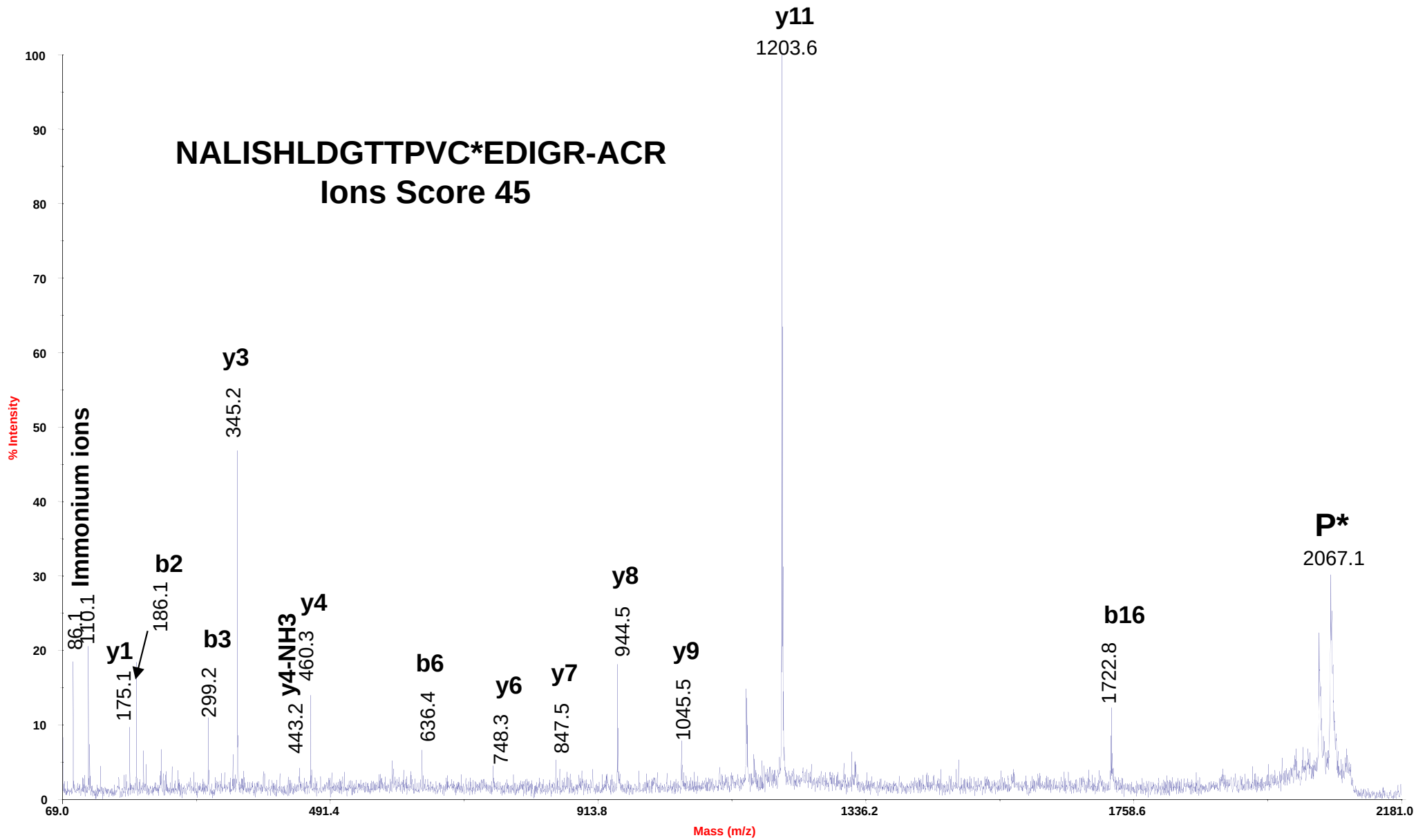

Figure S3-16,17,18

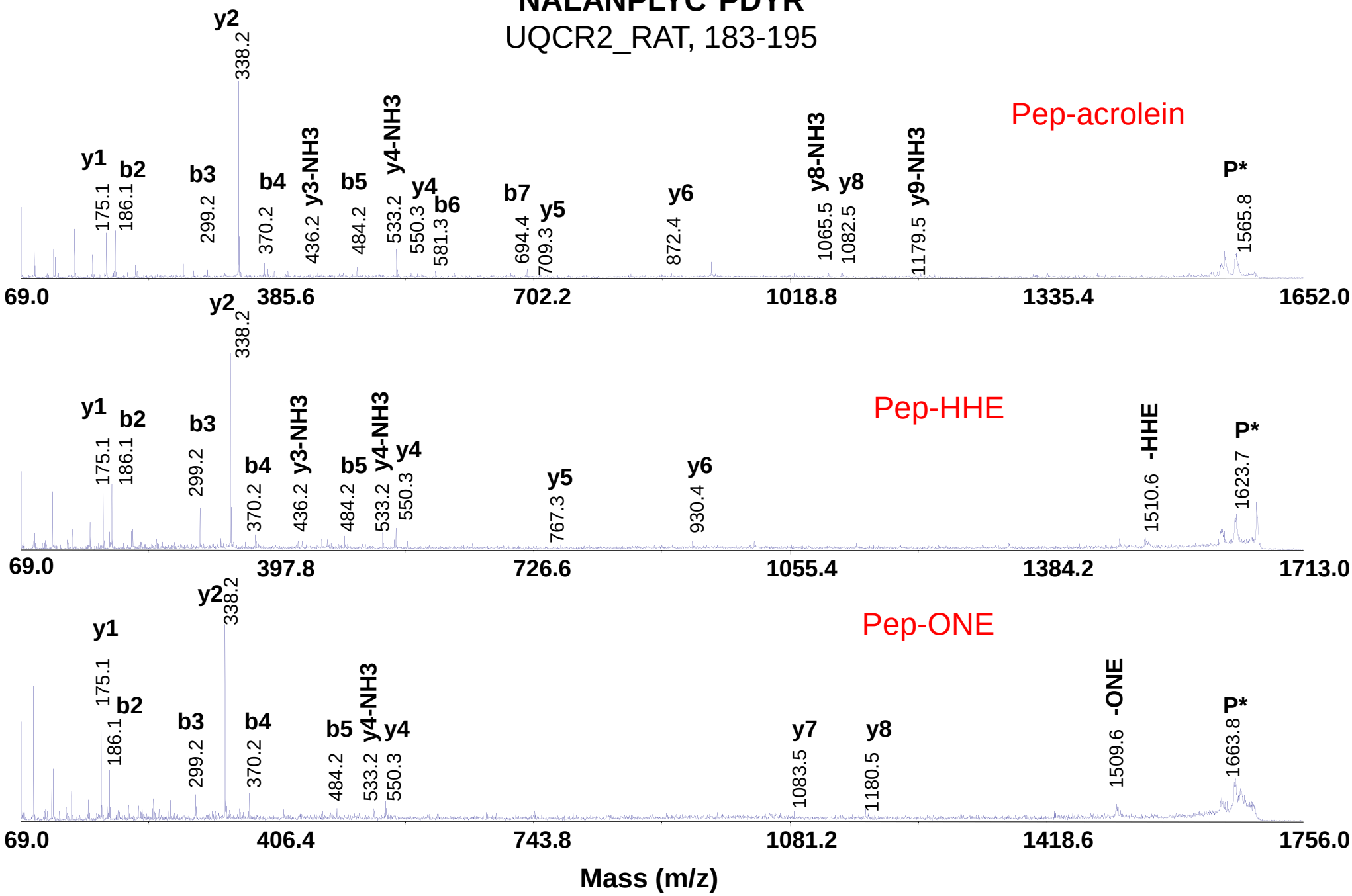

Figure S3-19
4700 MS/MS Precursor 1665.89

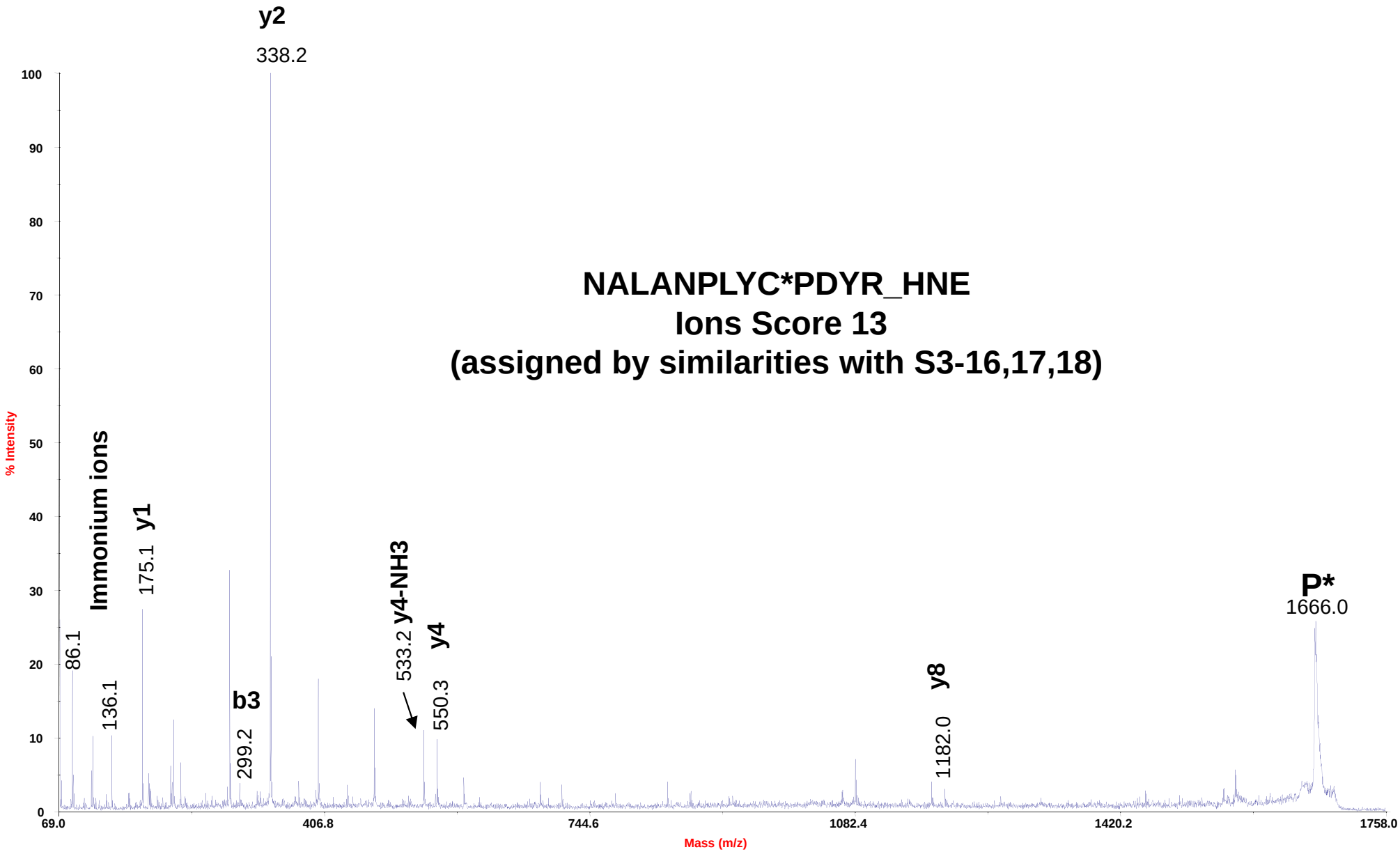

Figure S3-20
4700 MS/MS Precursor 1533.79

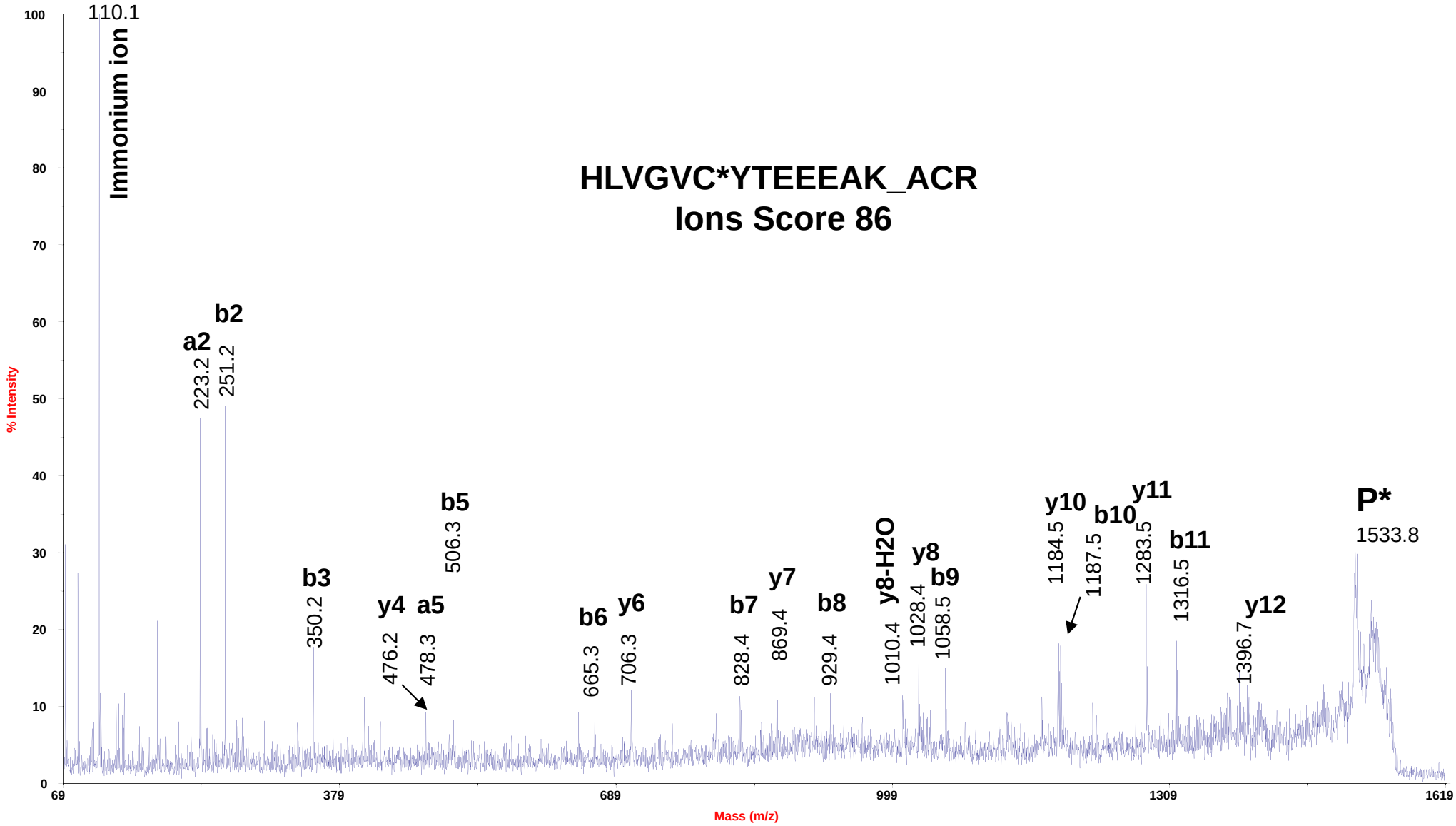

Figure S3-21
4700 MS/MS Precursor 1312.68

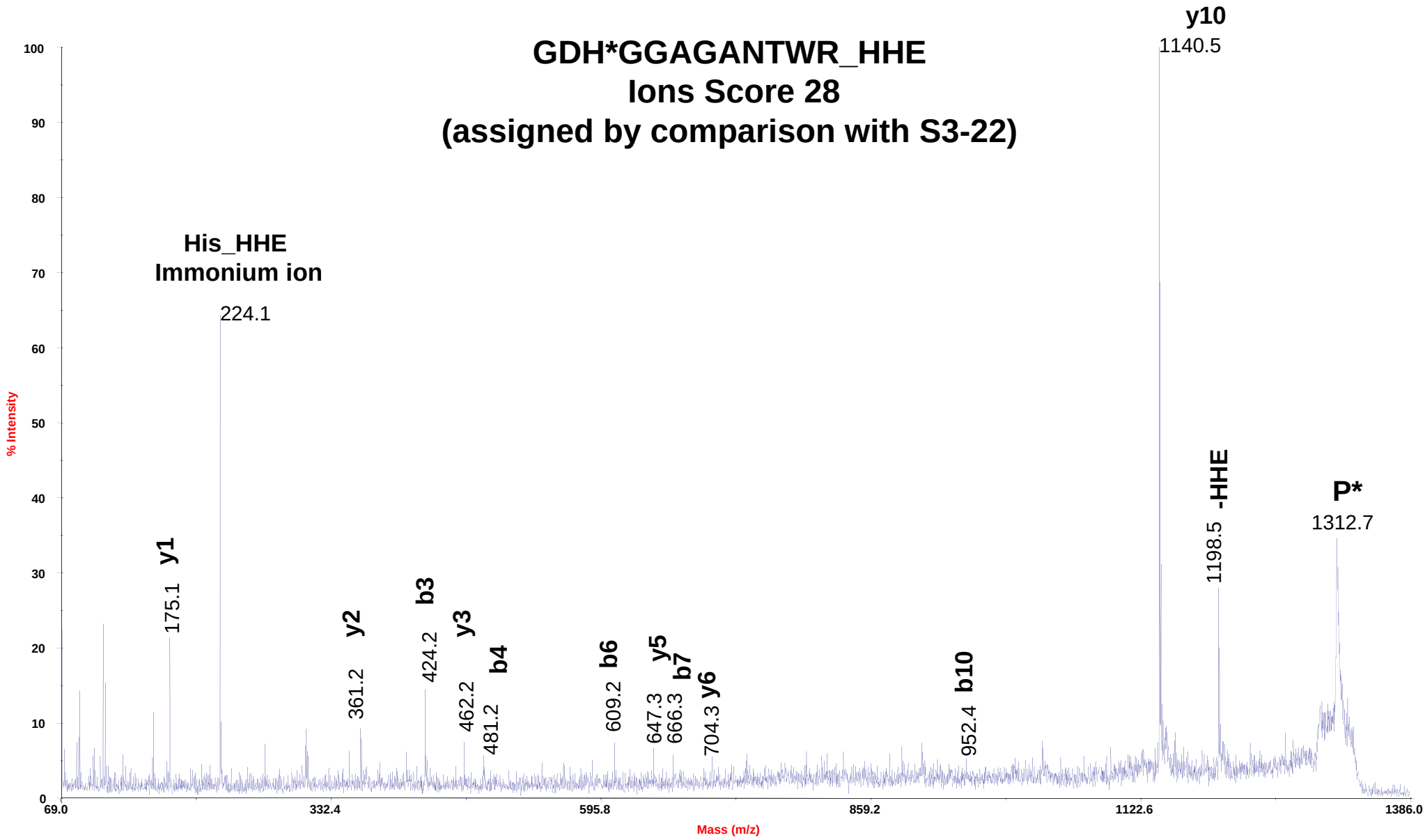

Figure S3-22
4700 MS/MS Precursor 1352.65

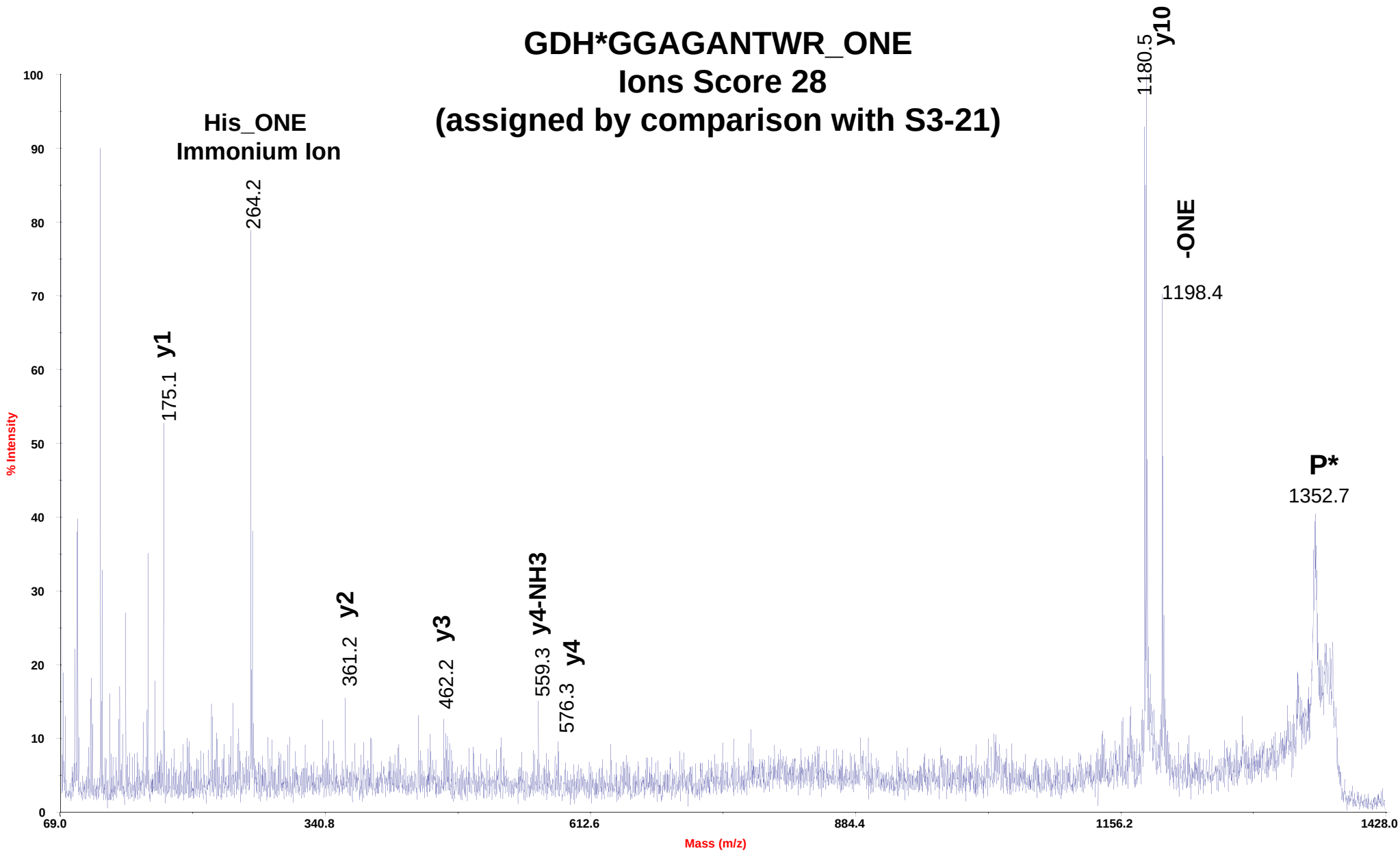

Figure S3-23
4700 MS/MS Precursor 1813.9

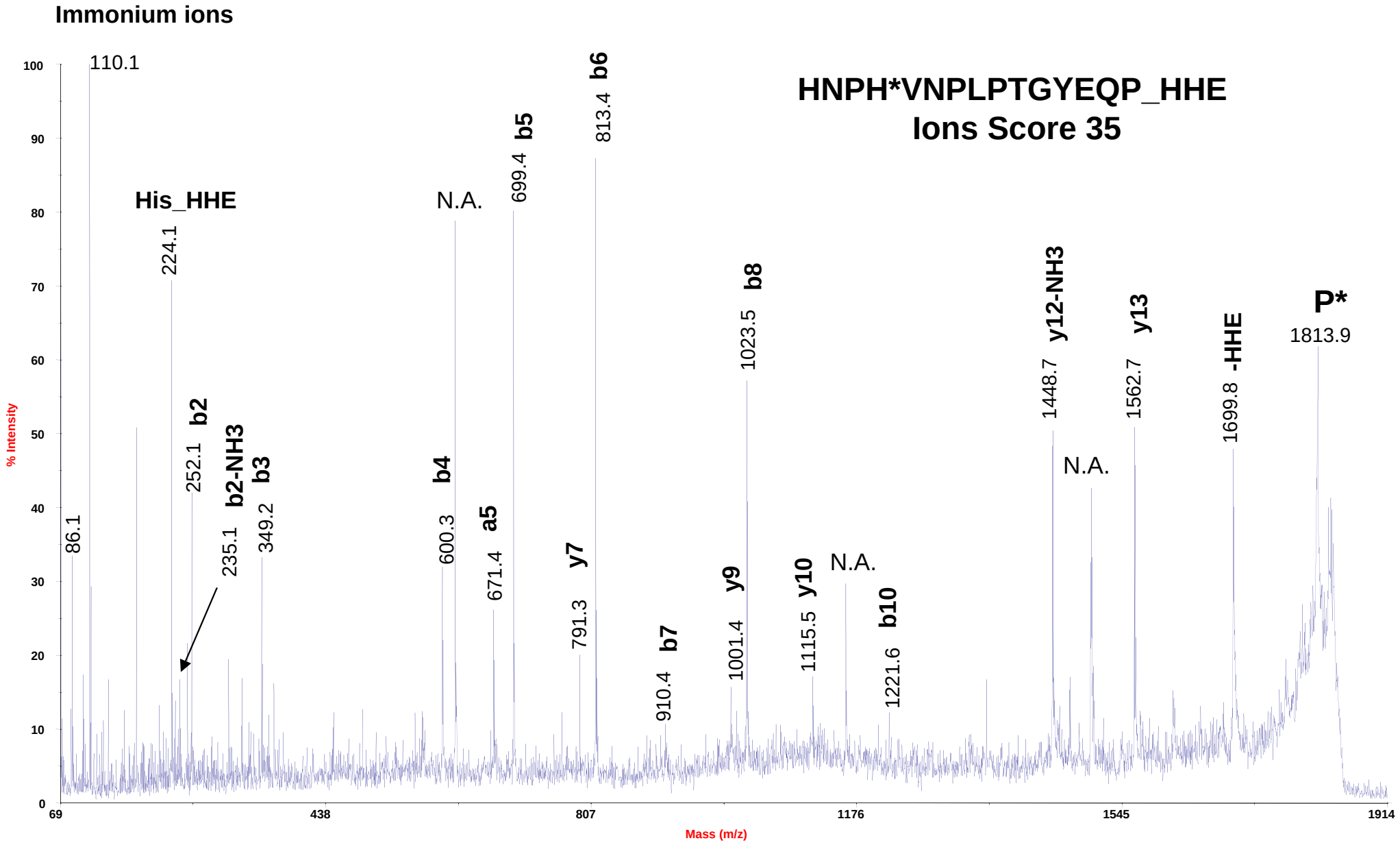

Figure S3-24
4700 MS/MS Precursor 1384.65

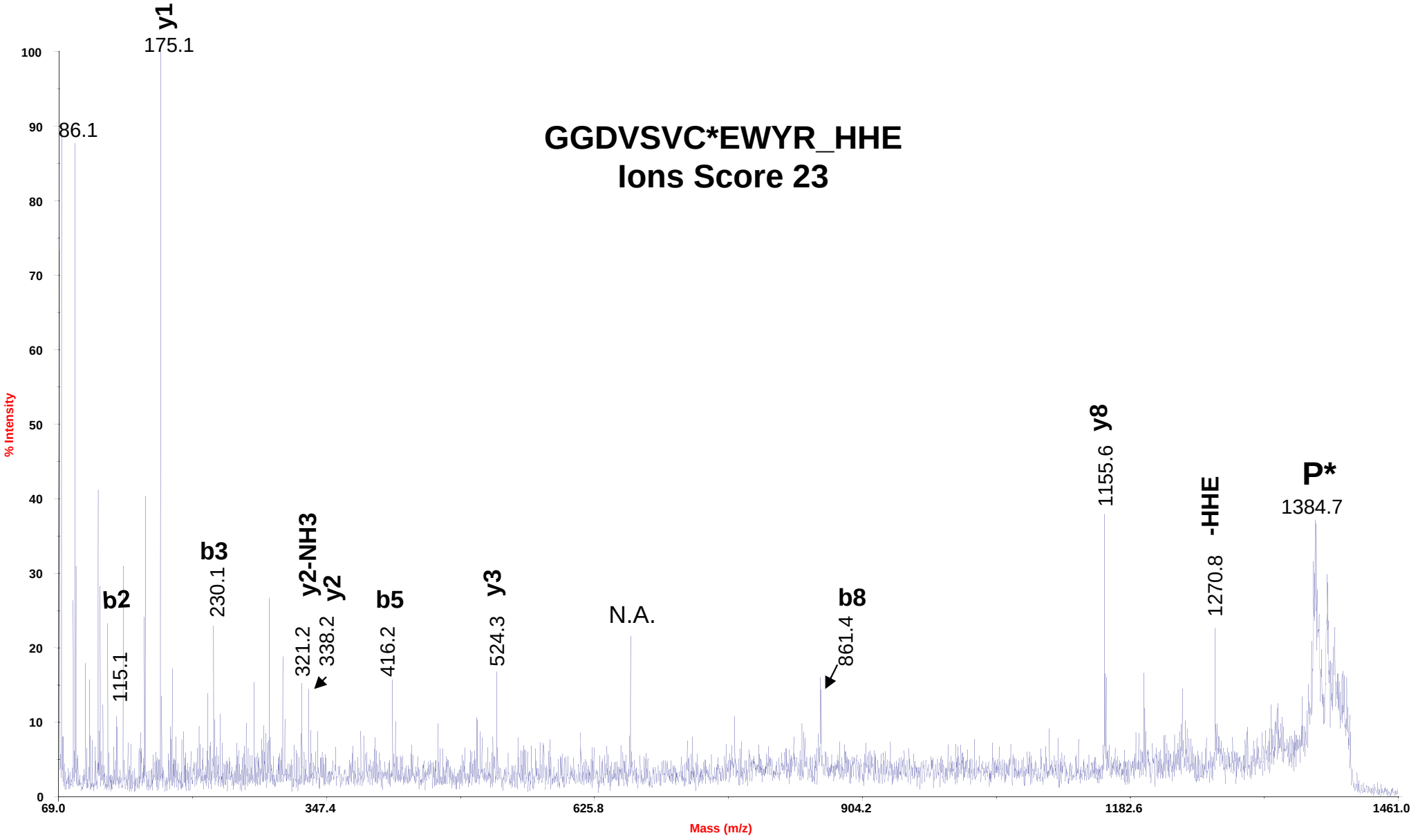

Figure S3-25
4700 MS/MS Precursor 1641.84

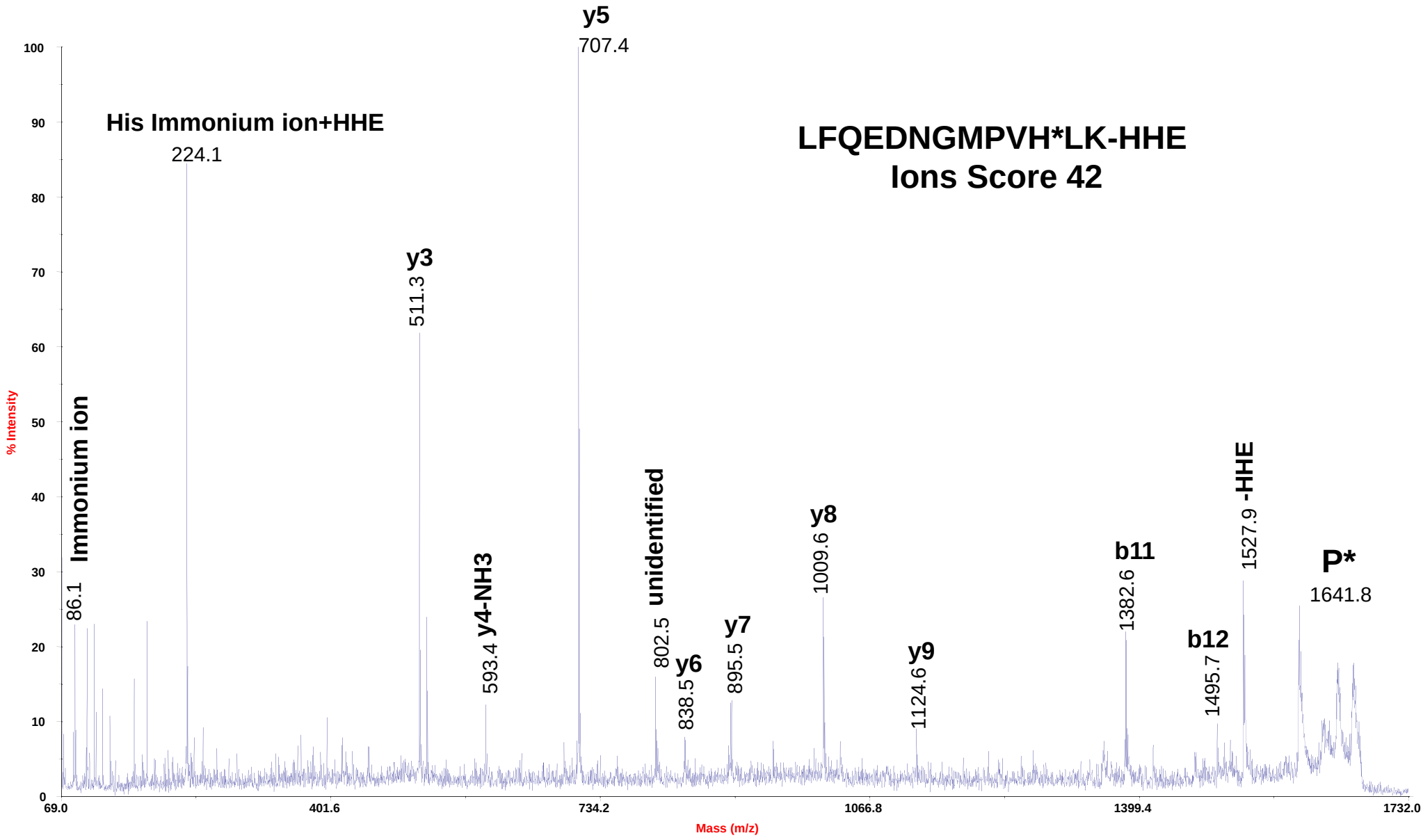

Figure S3-26
4700 MS/MS Precursor 1930.02

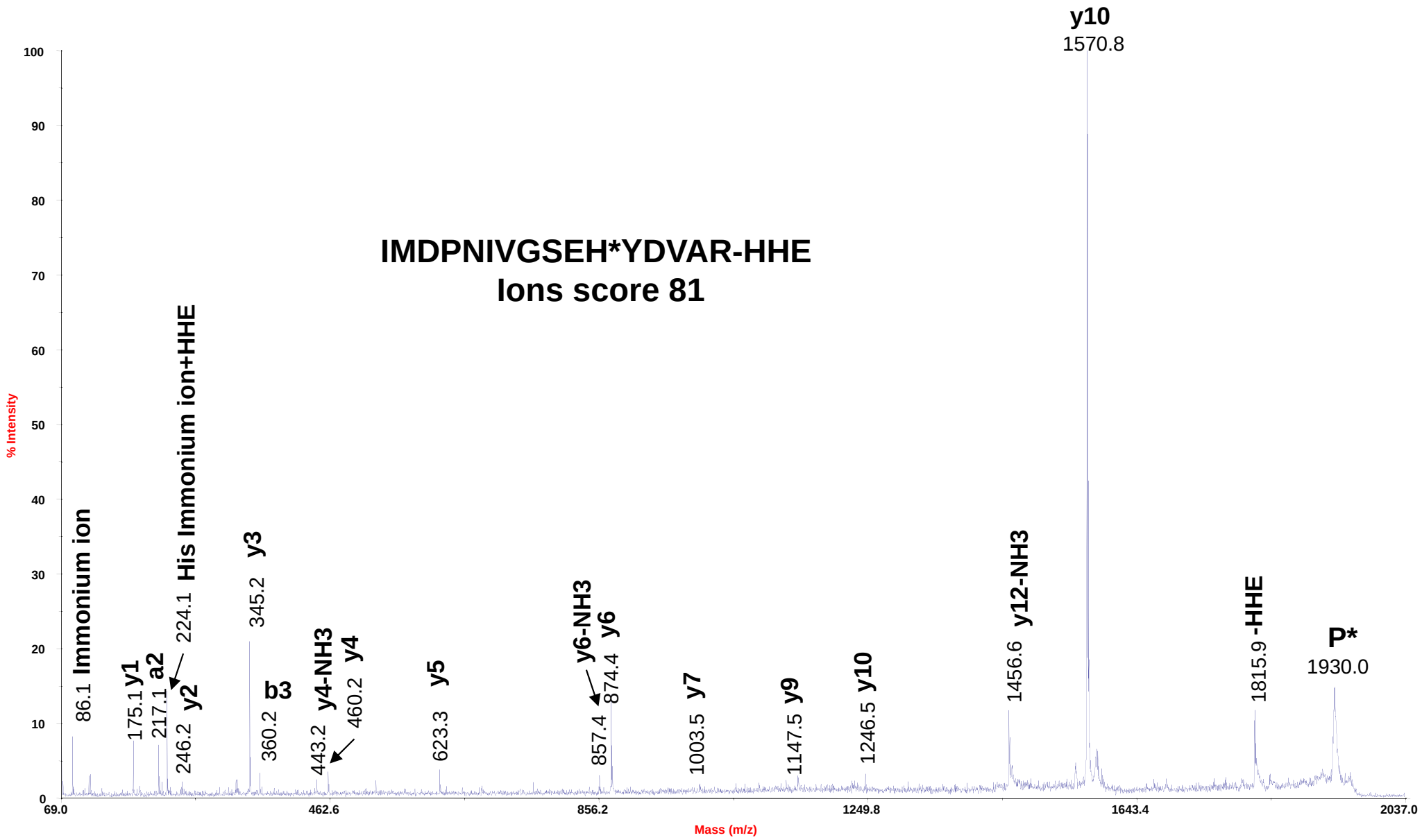

Figure S3-27
4700 MS/MS Precursor 2375.33

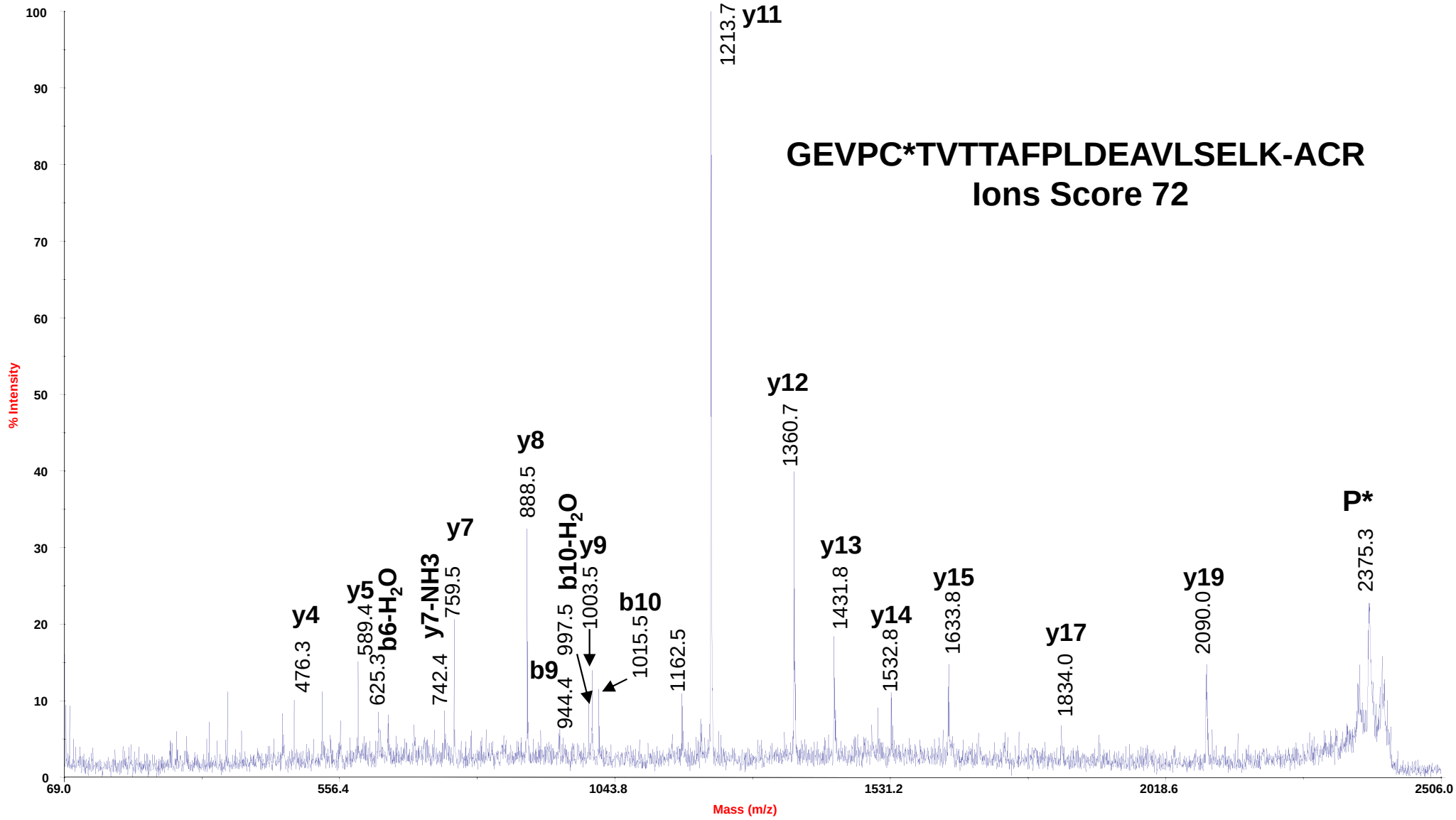

Figure S3-28
4700 MS/MS Precursor 2273.18

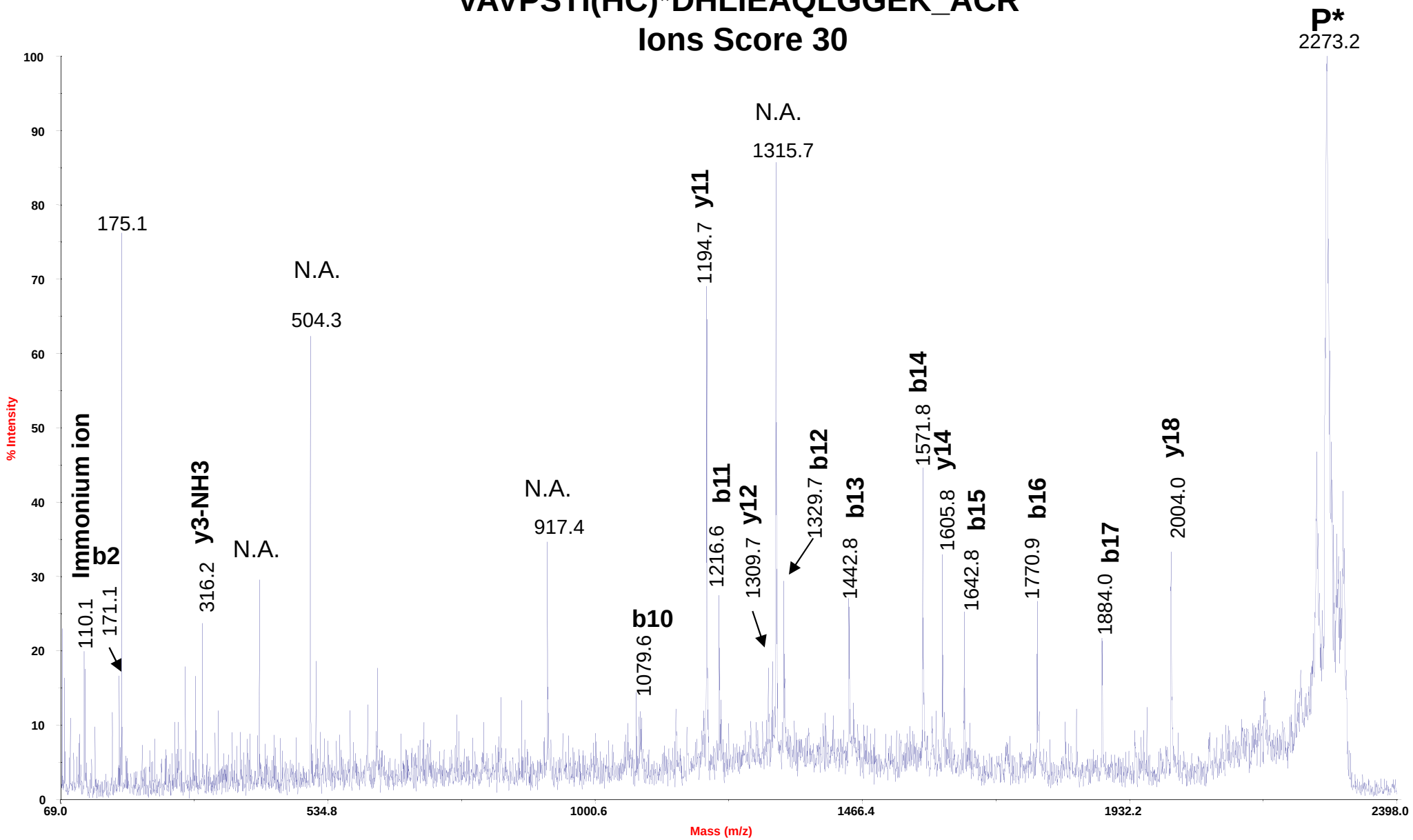

Figure S3-29
4700 MS/MS Precursor 1488.76

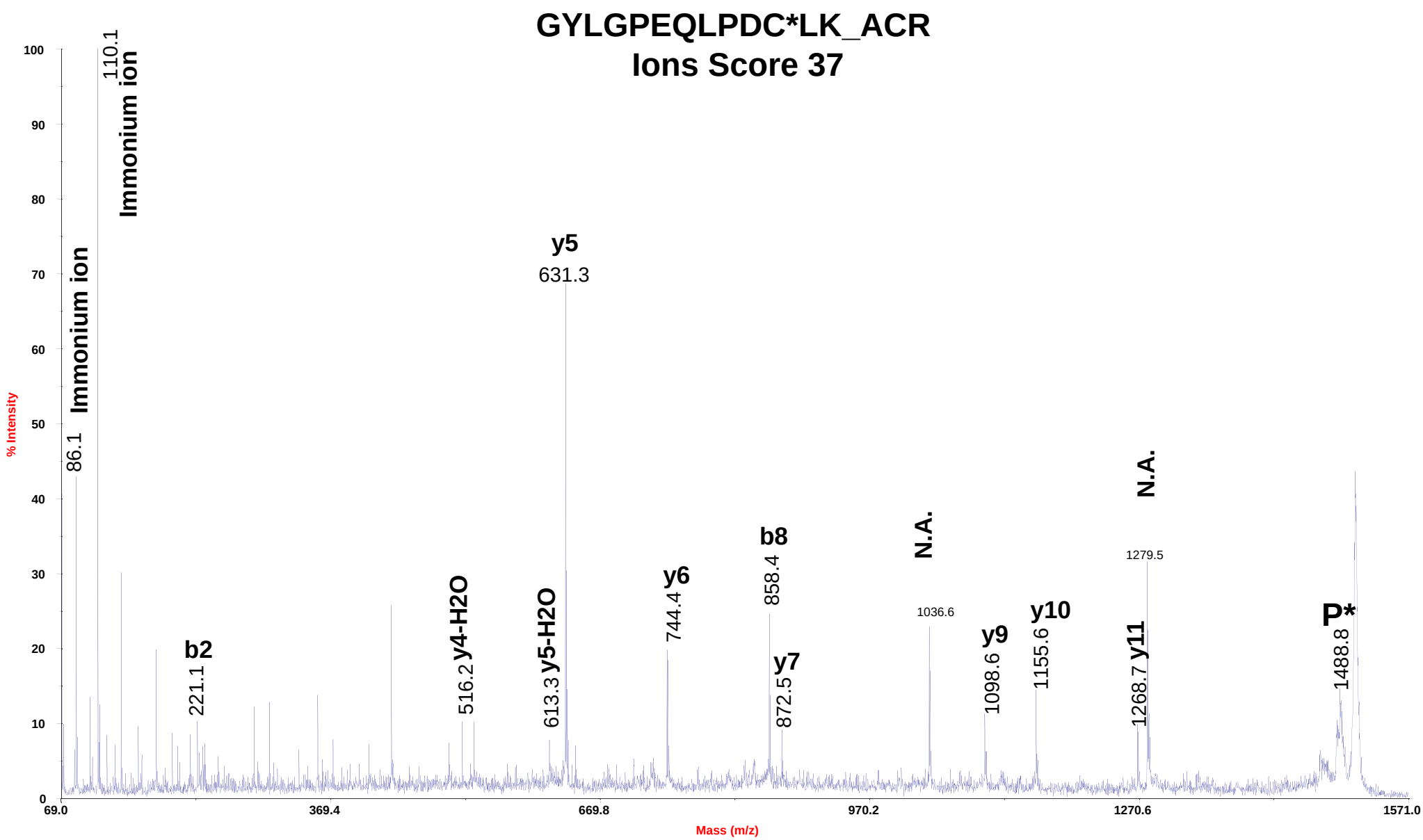

Figure S3-30
4700 MS/MS Precursor 1458.76

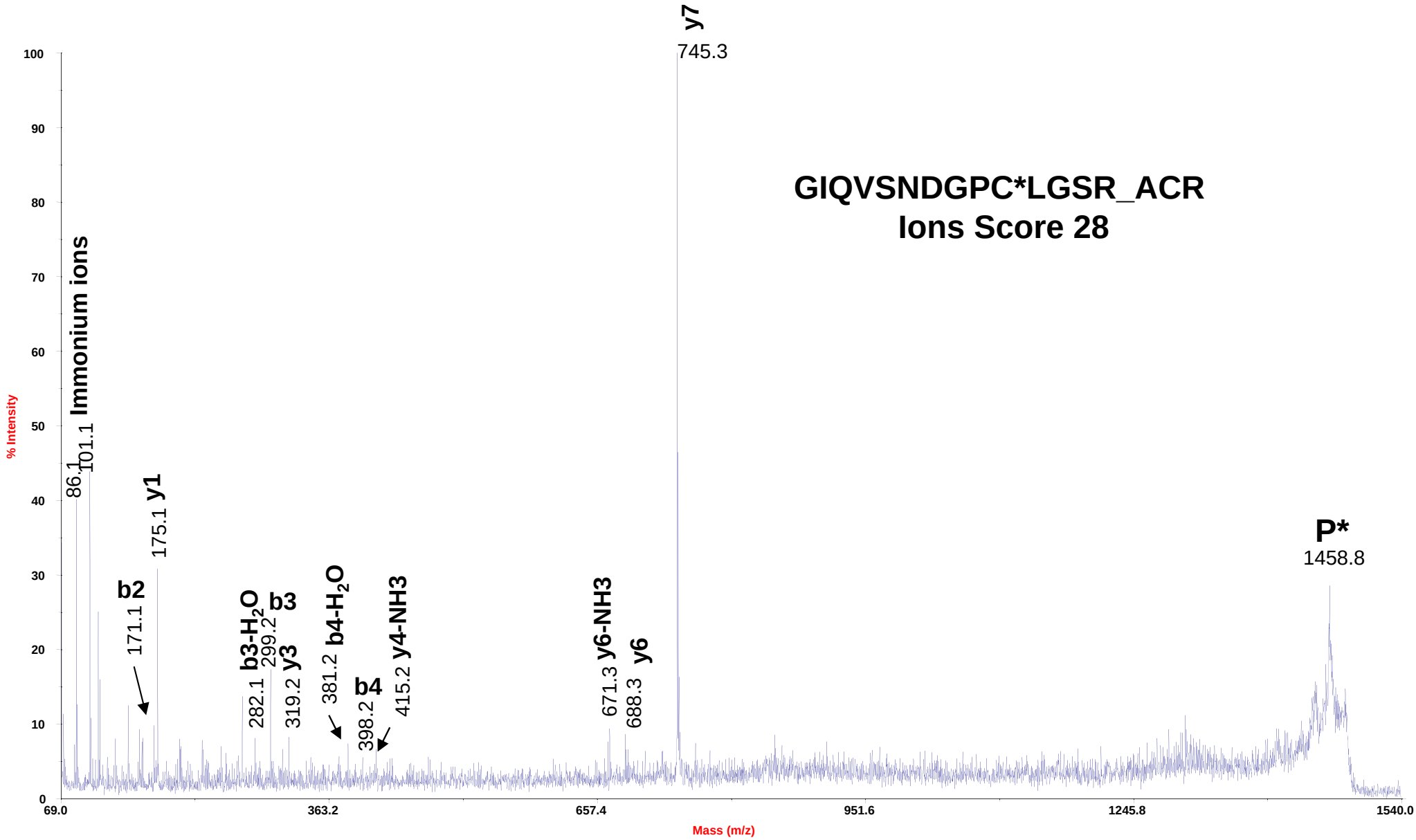

Figure S3-31
4700 MS/MS Precursor 1643.77

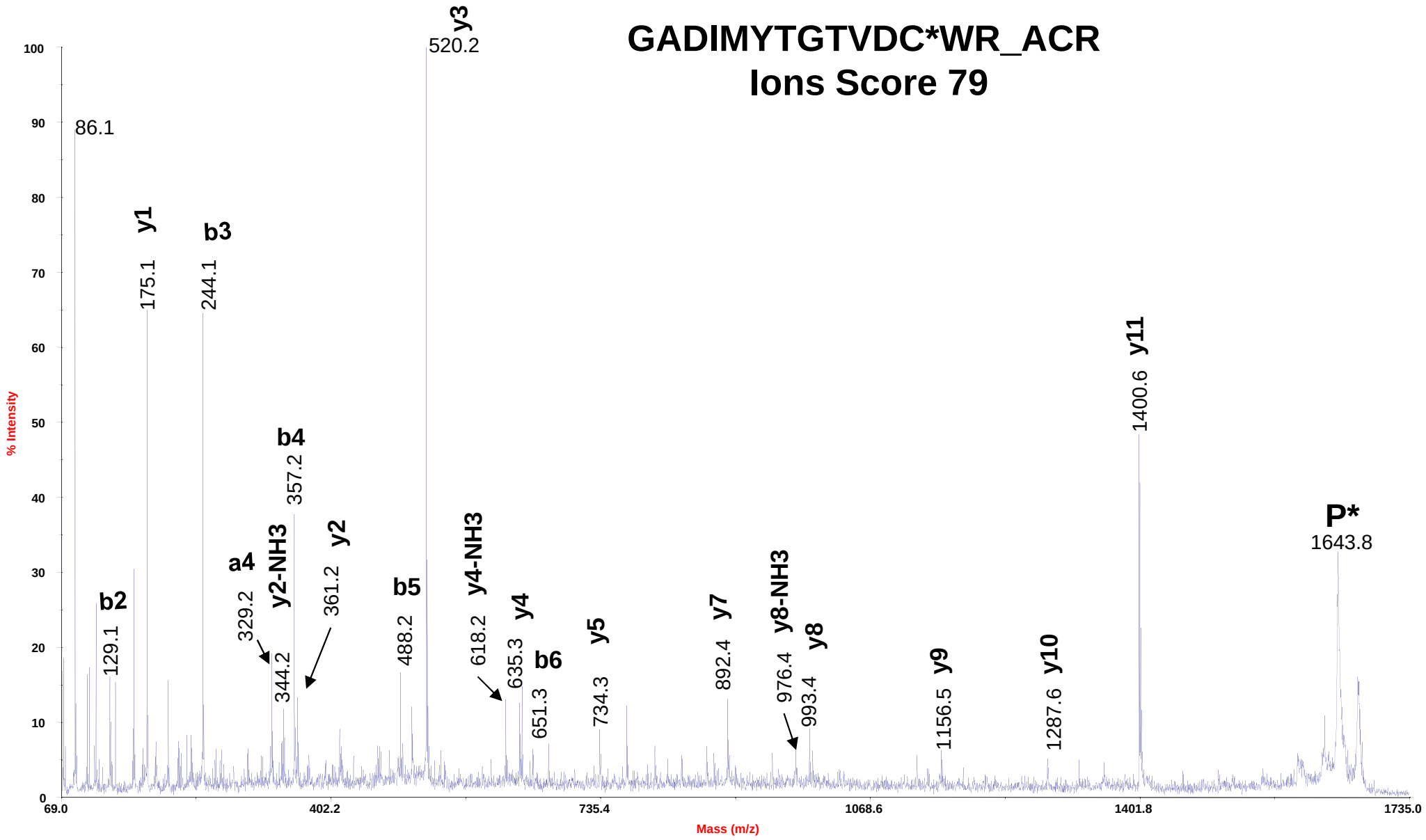

Figure S3-32
4700 MS/MS Precursor 1701.77

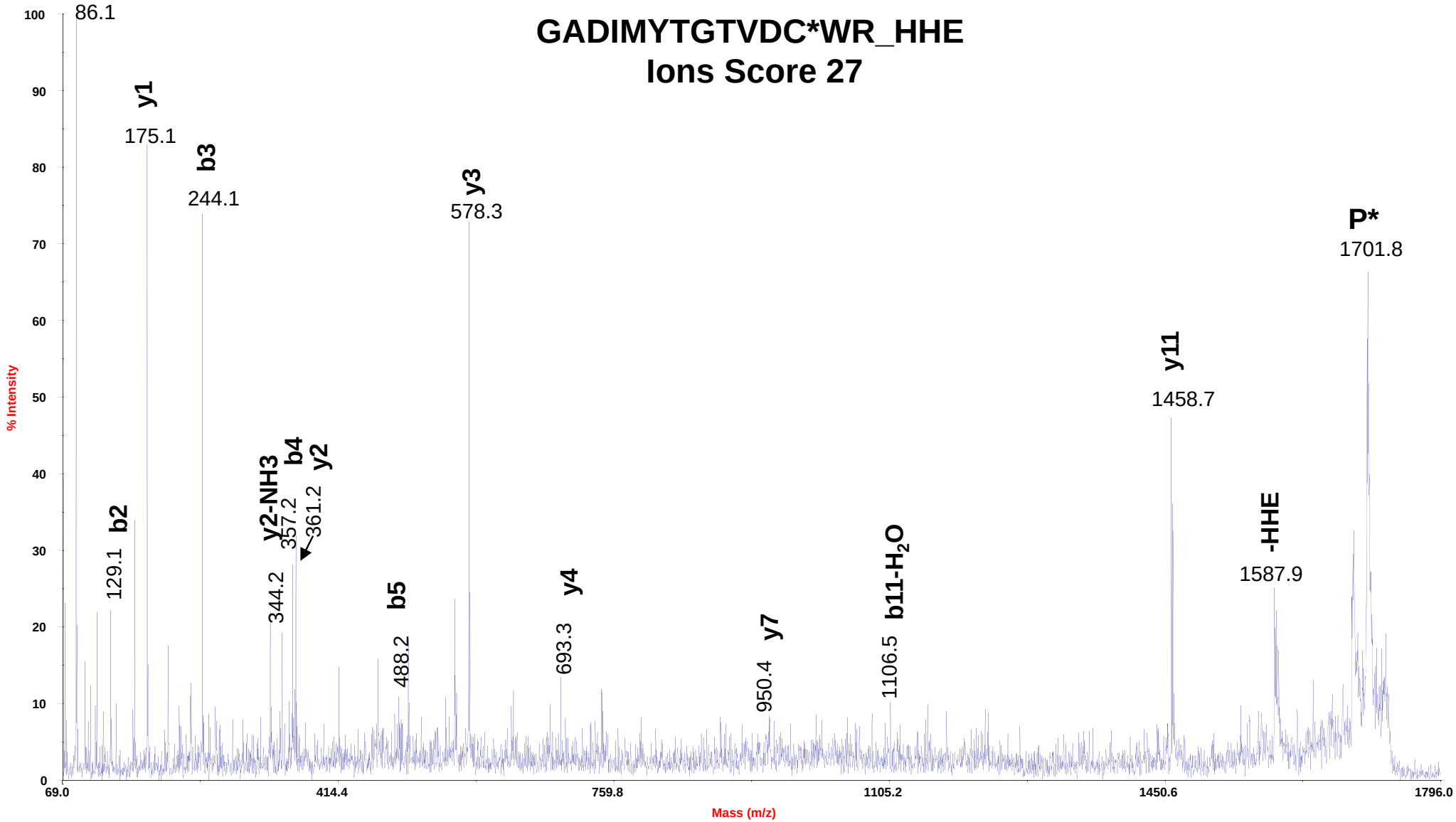

Figure S3-33
4700 MS/MS Precursor 1252.59

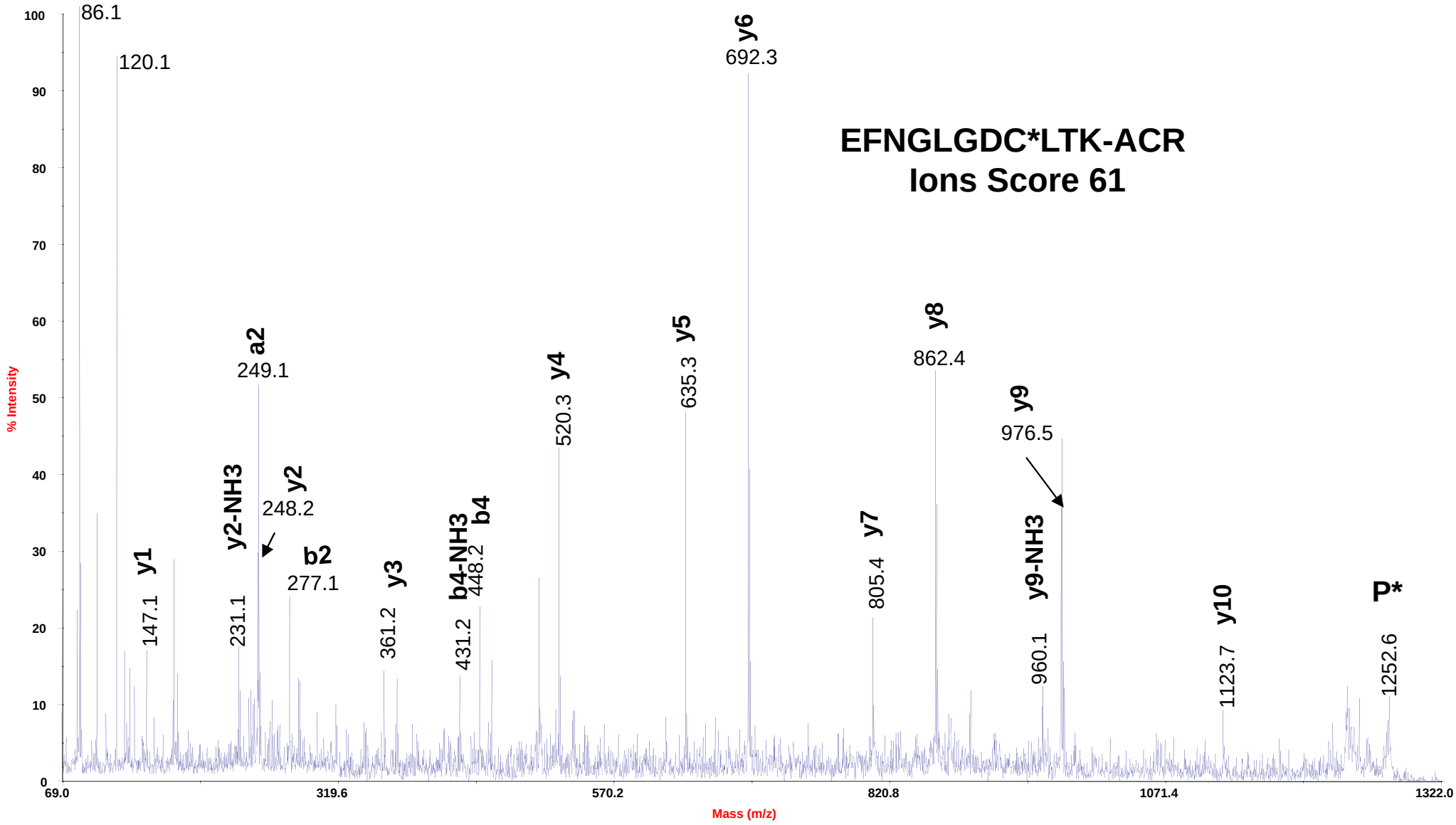

Figure S3-34
4700 MS/MS Precursor 2127.06